WATER-ROCK INTERACTION OF SILICIC ROCKS: AN EXPERIMENTAL AND GEOCHEMICAL MODELLING STUDY

Alejandro Rodríguez

Faculty of Earth Sciences
University of Iceland
2011

WATER-ROCK INTERACTION OF SILICIC ROCKS: AN EXPERIMENTAL AND GEOCHEMICAL MODELLING STUDY

Alejandro Rodríguez

60 ECTS thesis submitted in partial fulfillment of a
Magister Scientiarum degree in Geology

Advisor
Dr. Andri Stefánsson, University of Iceland

External examiner
Dr. Bergur Sigfússon, Reykjavík Energy

Faculty of Earth Sciences
School of Engineering and Natural Sciences
University of Iceland
Reykjavik, May 2011

Water-rock interaction of silicic rocks: an experimental and geochemical modelling study
Water-rock interaction of silicic rocks
60 ECTS thesis submitted in partial fulfillment of a *Magister Scientiarum* degree in Geology

Faculty of Earth Sciences
School of Engineering and Natural Sciences
University of Iceland
Askja, Sturlugata 7
101 Reykjavik
Iceland

Telephone: 525 4000

Bibliographic information:
Rodríguez, A., 2011, *Water-rock interaction of silicic rocks: an experimental and geochemical modelling study*. Master's thesis, Faculty of Earth Sciences, University of Iceland, pp. XX.

ISBN XX

Printing: Háskólaprent ehf.
Reykjavik, Iceland, May 2011

Abstract

The water-silicic rock interaction under geothermal conditions was studied both experimentally and using reaction path simulations to get insights into to the process of rock alteration including secondary mineralogy, water chemistry and mass transfer as a function of rock composition and reaction progress (ξ). The experiments and model calculations were conducted at 240°C and water vapour saturation pressures on two glass samples, dacite from Askja and rhyolite from Hekla, and initial non-thermal groundwater containing ~5000 ppm NaCl, ~1600-3500 ppm CO_2 and ~140 ppm H_2S. The dissolution of the silicic glasses were found to be incongruent with the formation of secondary minerals including quartz, anhydrite, clays like montmorillonite, illite and/or mixed illite-smectite and chlorite, zeolites like analcime and phillipsite as well as traces of anatase and fluorite. Moreover, most of the observed minerals were found to be saturated or supersaturated. The changes in water chemistry were characterized by a decrease in CO_2, Mg, Fe and Al concentrations, relatively steady concentrations for Na and SO_4 whereas Si initially rose followed by decrease after ~40 days. For H_2S, F and Ca considerable differences were observed depending on the starting material. The formation of secondary minerals greatly reduced the mobility of Al, Fe, Mg and Si and to lesser extent Ca and Na, however, K was observed to be mobile relative to B. The reaction path simulations demonstrate that the appearance of various secondary minerals in a closed system is a function of reaction progress, initially with the formation of clays and sulphides followed by the appearance of quartz and zeolites. Upon considerable reaction (>1 mol rock dissolution in 1 kg of water) other Al-Si minerals also become important and sometimes predominant including epidote, feldspars and chlorite, this last stage closely corresponds to the commonly observed alteration mineralogy associated with geothermal systems hosted by silicic rocks. The exact clay mineralogy was also found to be dependent on the initial system composition, with illite and mixed illite-smectite being more important associated with the rhyolite and montmorillonite associated with the dacite. In addition, comparison of the experimental results and reaction path simulations revealed that reaction kinetics may be of potential importance in the formation of Na, K and Si containing minerals with some profound influences on the respective elemental solution concentrations. This in turn affected the predicted geothermometry temperatures that were found to vary from <150 to >350°C and be a function of the extent of reaction for the 240°C experiments.

Útdráttur

Samspil jarðhitavatns og súrs bergs var skoðað með tilraunum og með notkun líkanreikninga til að bæta innsýn á áhrif bergsamsetningar og uppleysingarmagns á ummyndunarferlið og efnasamsetningu vatnsins. Tilraunirnar og líkanreikningarnir voru gerðir við 240°C og gufuþrýsting vatns á tveimur sýnum, dasíti úr Öskju og rýólíti frá Heklu, og köldu grunnvatni sem bætt var við um 5000 ppm NaCl, ~1600-3500 ppm CO_2 og ~140 ppm H_2S. Uppleysing og ummyndun súrs bergs leiðir til myndunar ummyndunarsteinda eins og kvars, anhýdríts, leirs eins og montmórillóníts, illíts, blandleirs og klóríts, geislasteinda eins og analsíms og phillipsíts ásamt anatasi og fluoríti. Flestar þessarra steinda voru jafnframt mettaðar og/eða aðeins yfirmettaðar. Styrkur CO_2, Mg, Fe og Al lækkaði með tíma á meðan styrkur Na og SO_4 hélst nokkuð stöðugur og styrkur Si hækkaði og lækkaði síðan eftir um 40 daga. Styrkur H_2S, F og Ca var nokkuð breytilegur. Af þessu leiðir að myndun ummyndunarsteinda lækkaði hreyfanleika margra efna eins og fyrir Al, Fe. Mg og Si á meðan Ca, Na og K voru mun hreyfnalegri. Niðurstöður líkanreikninganna benda til að myndun einstakra ummyndunarsteinda og styrkur efna í vatnslausn sé háður uppleysingarmagni súrs bergs. Við litla uppleysingu myndast leir og jafnvel súlfíð og síðan kvars og geislasteindir. Við nokkra uppleysingu bergs (>1 mól berg í 1 kg vatni) myndast síðan steindir eins og epídót, feldspöt og klórít, sem eru algengar steindir í náttúrlegum jarðhitakerfum við 250°C. Gerð leirsteinda reyndist einnig vera nokkuð háð samsetningu súra bergsins, þar sem ummyndun á ríólíti leiddi til myndunar á illíti, blandleirs og klóríts á meðan montmórillónít og klórít var algengari tengt ummynduna á dasíti. Samaburður á niðurstöðum tilraunanna og líkanreikninganna bendir einnig til þess að efnahvarfahraði geti skipti máli við jarðhitaaðstæður ekki síst tengt myndun Na, K og Si ríkra steinda sem hefur áhrif á efnastyrk vatnsins. Slíkt hafði áhrif á niðurstöður reikninga á hitastigi út frá efnahitamælum sem gáfu til kynna að hitastig vatnsins væri á bilinu <150 til >350°C og breyttist með tíma fyrir tiltekin efnahitamæli.

Dedicated to my parents, Hernán Rodríguez and Beatriz Badilla

Table of contents

List of figures

List of tables

Acknowledgements

I would like to express my gratitude to the UNU-GTP Programme for the economical support in this project. Special thanks to the director Dr. Ingvar Friðleifsson for gave me the opportunity to come back to Iceland and enrol the master´s programme. I also received a valuable help from other staff members like Lúdvík Georgsson, Dorthe Holm, Þórhildur Ísberg, and Markus Wilde. I am very grateful with the great support and teachings from my supervisor, Andri Stefánsson. He has the gift of explaining difficult things in easy ways. My special appreciation to Alexandre P. Gysi for teaching me all that I know about high temperature experiments and how to deal with numerous problems associated to them. Þorsteinn Jónsson had an extraordinary patience with me and with some problems with the equipments. Nicole Keller helped me with the ICP analysis and her suggestions on data handling were important. Comments on how to improve this work also came from Þráinn Friðriksson (ÍSOR). I am in great dept with Domenik Wolf-Boenisch and Sigurður Gíslason, from the Faculty of Earth Sciences, who generously provided the rock samples utilized in the experiments. Níels Óskarsson, from the Faculty of Earth Sciences, assisted me in analyzing the composition of secondary minerals with XRD techniques and with valuable discussions. Sigurður Jónsson, from ÍSOR, helped me with the analysis of alteration minerals as well. Birgir Jóhanesson, from the Innovation Centre Iceland, kindly helped me preparing the samples for the SEM sessions and with the operation of the equipment. Sigurður Markússon gave me a valuable assistance in identifying minerals in the SEM. Finally, greatest gratitude to my co workers in the aqueous geochemistry group: Kevin Padilla, Ásgerður Sigurðarsdóttir, Samuel Scott, Júlía Björke, Hanna Kaasalainen and Nicole Keller. Their scientific and moral support was highly appreciated.

1 Introduction

Geothermal alteration results from interaction between hot fluids and rocks. The study of geothermal alteration itself can provide valuable information on the processes of interaction including rock and fluid composition and alteration temperature (e.g. Browne, 1978; Elders et al., 1981; Henley and Ellis, 1983; Bird et al., 1984; Lesher et al., 1986; Sveinbjörnsdóttir et al., 1986; Henneberger and Browne, 1988; Palmer and Edmond, 1989; Lonker et al., 1990; Reyes, 1990; Franzson, 2002; Davis et al., 2003; Marks et al., 2010). Even though the primary rock type is an important factor, its effect on geothermal alteration is considered less important compared with permeability, temperature and fluid composition (Henley and Ellis, 1983) For example, Browne (1978) noted that at 250–280°C quartz, albite, K-feldspar, chlorite, Fe-epidote, illite, calcite and pyrite were the predominant alteration minerals in basalt, sandstones, rhyolites and andesites. Yet, there are some important differences between mafic and silicic rock alteration assemblages.

The geothermal alteration of basalts and the formation of secondary minerals at low temperatures are commonly dominated by phyllosilicates, zeolites, oxides and hydroxides and sometimes carbonates (e.g. Kristmannsdóttir and Tómasson, 1978; Kristmannsdóttir, 1979; Mehegan et al., 1982; Schiffman and Fridleifsson, 1991; Neuhoff et al., 1999;Weisenberger and Selbekk, 2009). With increasing temperature, these are replaced by zone of mixed clays at 200-250°C, chlorite-epidote at 250-300°C and epidote-actinolite at >300°C (e.g. Schiffman and Fridleifsson, 1991). The main zeolites observed at <150°C include analcime and wairakite with other minerals including chalcedony and quartz, K-feldspar, smectites and chlorite, calcite, prehnite, epidote, pyrite and actinolite (e.g. Kristmannsdóttir, 1979; Hreggvidsdóttir, 1987; Schiffman and Fridleifsson, 1991; Lonker et al., 1993; Larsson et al., 2002). For andesitic and silicic rock compositions, a similar pattern is observed with some differences especially in the clay mineralogy. At low temperatures, clays, including kaolinite and smectites predominate. With increasing temperature zeolites like wairakite and analcime, chlorite, mixed illite-smectite minerals and micas, epidote, calcite, pyrite and amphibole become important (e.g. Browne, 1978; Lonker et al., 1990; Reyes, 1990; Mas et al., 2006). The clays formed during geothermal alteration of silicic rocks are much more Na and K rich compared to basalts typically consisting of mixed illites-smectites and montmorillonites. Additionally, the chlorites are often more Fe-rich and Mg-depleted resulting from low Mg content of andesites, dacites and rhyolites compared to basalts (Inoue and Utada, 1983; Bethke, 1986; Harvey and Browne, 1991; Altaner and Ylagan, 1997; Inoue et al., 2004; Mas et al., 2006).

Based on data on natural geothermal fluids it has been concluded that local equilibria between geothermal minerals and the fluids control the concentrations of major components in the fluids, except mobile elements like Cl, at temperatures as low as 50°C (e.g. Ellis, 1970; Giggenbach, 1980, 1981; Arnórsson et al., 1983; Stefánsson and Arnórsson, 2000; Stefánsson and Arnórsson, 2002). The reason for this is twofold. Firstly, as demonstrated for Icelandic geothermal systems two types of fluids recharge the systems, saline and meteoric, yet despite the variable elemental concentrations at a particular temperature, the relative concentration is the same with respect to major elements. Secondly, based on the Phase Rule and assuming pressure effects on the reactions to be insignificant, only two parameters are needed to describe a system, temperature and one

component, notably Cl concentration. As a result, secondary mineral assemblages show various temperature dependences depending on their thermodynamic stability fields.

The geothermal alteration of rocks involves the dissolution of primary minerals and glasses and the formation of secondary minerals and dissolved solutes in water. In a closed system of fixed composition, the overall reaction is incongruent and is affected by temperature, rock and fluid composition and extent of reaction. Moreover, for systems containing more than one phase, the extent of reaction will further result in changes in mass between the various phases. The result is that the process of alteration of a chemical system of fixed composition (rock and fluid) must be influenced by several factors including temperature, reaction progress and reaction mechanism (Helgeson, 1968; Helgeson, 1979; Marini, 2006). However, the contribution of the various factors is somewhat unclear. Many studies have considered the thermal conditions the predominant factor during geothermal alteration of a given rock and fluid system, not least reflected in the clay composition and mineralogy (e.g. McDowell and Elders, 1980; Inoue and Utada, 1983 Cathelineau and Nieva, 1985; Ji and Browne, 2000). However, several authors have pointed out that other factors are also important including very fine variations in fluid and rock composition, time or fluid-rock ratio (extent of reaction), and the nature of the precursor conditions for nucleation and crystal growth (e.g. Roberson and Lahann, 1981; Lonker et al., 1990; Beaufort et al., 1992; Essene and Peacor, 1995; Dolejs and Wagner, 2008; Stefánsson, 2010; Gysi and Stefánsson, 2011).

Most of the attempts at delineating the relative importance of the numerous processes likely to affect the composition of both fluids and minerals are based on the assumption of local equilibrium (Helgeson, 1979; Giggenbach, 1984; Nordstrom and Munoz, 2006). For such systems, a given aqueous solution is in equilibrium with the saturated secondary minerals whereas the primary phases are unstable. Consequently, mass movement in the system is regarded to be driven by irreversible dissolution of the primary mineral and the overall energy of the system approaches minimum Gibbs free energy at a given temperature and pressure. Chemical mass transfer modelling is a numerical approach to predict the progress of multicomponent fluid–rock reactions using data on the thermodynamics and kinetics of the reactions of interest. In practice, there are mainly two problems in the application of such models for studying mass transfer of natural systems. Firstly, the geometry of the system needs to be adjusted to the chemical and geological system of interest (Heinrich et al., 1996) and secondly, the conceptual geochemical model and the thermodynamic and kinetic database must include the key reactions under the relevant T-p-x conditions (Marini, 2006). Both these criteria are often not met and/or difficult to constrain However, reaction modelling can give important insight into the fine details of fluid-rock interaction that is often difficult to do by studying natural systems, particularly the effects of extent of reaction (time) and system composition at isothermal conditions, processes that are probably underestimated as major factors in natural fluid-rock systems.

The approach adopted in this study is to gain insight into the processes of water-rock interaction and the effects of reaction progress on fluid composition and secondary mineralogy at a given temperature, consisted of combining and comparing reaction path simulations with laboratory experiments. In this study, we report the results of silicic rock alteration at 240°C. Batch type experiments were carried out as a function of time and the alteration mineralogy and water chemistry studied and compared with the results of reaction path modelling.

2 Materials and methods

2.1 Materials and sample preparation

Two silicic volcanic samples were selected for the present study. The first sample (A75) was from the 1875 Askja eruption and is well characterized (Sigvaldason et al., 1981; Sparks et al., 1981; MacDonald et al., 1987; Larsen et al., 1999; Sigvaldason, 2002; Jónasson, 2007). The second sample (H3W) is from the 2900 BP Hekla eruption (Sigvaldason, 1973; Jónasson, 2007). Additional details of the glasses are given by Wolff-Boenisch (2004) and Wolff-Boenisch et al. (2004). The chemical composition of the samples is given in Table1. According to the silica versus alkali content of the rocks (Le Bas et al., 1986), samples A75 and H3W are categorized as dacite and rhyolite, respectively.

Samples were reduced in size from hand specimens to chips using a ~1.6 kg hammer. During this process the samples were kept inside thick plastic bags in order to prevent metal debris contamination from the hammer. Subsequently, the chunks were further grounded in a jaw crusher to particle sizes smaller than 2 mm. The grain fractions from 45 to 125 μm were separated from the bulk material with the aid of stainless steel sieves. Yields from raw materials were 24% and 22% for the A75 and H3W samples, respectively. The 45-125 μm fractions were washed with deionised water and finer particles were separated by floatation. Finally, the materials were dried at 50°C for 24 hours.

The starting solution consisted of water from Vellankatla spring, Thingvallavatn, Iceland (Gysi and Stefánsson, 2011) that were spiked with ~5000 ppm of NaCl. Prior to the experiments, the solutions were de-aired by bubbling N_2 gas thought the solutions for >30 minutes. Moreover, the experimental solutions were supplied with CO_2 gas and $Na_2S•9H_2O$ prior to heating. The compositions of the starting solutions are given in Table 2.

2.2 Experimental setup and procedure

Closed system reaction path experiments were carried out in 600 ml titanium Parr® type reactors equipped with a stirring mechanism and temperature controller. The pressure was measured using an Omega® model DP25B-E-230 pressure transducer connected to the system. To prevent degassing upon sampling, a special sampling setup was used consisting of a high pressure switch valve with 1.00 ml sampling loop connected to the sampling outlet of the reactor and to a HPLC pump for eluting the sample. The experimental equipment and the sampling line are shown in Figure 1.

Prior to the experiments, all the titanium wetted parts of the reactor system were cleaned mechanically, followed by a cleaning with 0.6 M HCl and sometimes also 5 M NaOH, washed with de-ionised water and eventually baked at ~450°C for 24 hours to form an inert TiO_2 oxide surface.

Table1. Chemical composition of the starting solid materials from Hekla and Askja used in the experiments.

Sample	**Hekla 3W**[a]	**Askja 1875**[a]
	H3W	A75
SiO_2 (wt.%)	69.79	69.28
TiO_2	0.21	0.9
Al_2O_3	13.79	12.42
Fe_2O_3	1.15	2.48
FeO	2.32	2.09
MnO	0.11	0.1
MgO	0.11	0.97
CaO	2.08	2.81
Na_2O	4.83	3.74
K_2O	2.48	2.21
P_2O_5	0.04	0.19
LOI	1.9	1.7
F[b] (ppm)	2080	2080
Cl[b]	7000	7000
B[b]	47	47

[a] Wolff-Boenish et al. (2004).
[b] Estimated, see chapter 4.

Table 2. The initial water compositions of the experiments. Units are in ppm.

Experiment	**Askja 1875 94-days**	**Askja 1875 30-days**	**Hekla H3W 42-days**
pH_T[a]	4.03	4.29	4.15
SiO_2	15.4	15.4	15.4
B	0.043	0.043	0.043
Na	2169	2164	2158
K	0.47	0.47	0.47
Ca	2.85	2.85	2.85
Mg	0.92	0.92	0.92
Fe	0.01	0.01	0.01
Al	0.03	0.03	0.03
CO_2	3491	1630	2482
H_2S	143	139	135
SO_4	1.44	1.44	1.44
Cl	3037	3037	3037
F	0.04	0.04	0.04

[a] Calculated based on charge balance.

The rector was loaded in the following manner. First, the solid sample and sodium sulphide were added to the reaction vessel and then it was closed and pressurised with CO_2 gas. The degassed starting solution was subsequently pumped into the vessel using an HPLC pump until the desired volume was reached and the reaction vessel heated to the set temperature. The whole procedure was conducted within 2 hours.

All the experiments were carried out at 240°C and at pressures close to the saturation water vapour pressure. Two experiments were carried out on the Askja sample (A75) lasting 94 and 30 days and one experiment on the Hekla sample (H3W) lasting 42 days. Details of the initial experimental setups are given in Table 3.

Water samples were collected at regular intervals during the experiments and the secondary mineralogy studied at the end of each experiment. For each water sample, four aliquots were collected. The first and second aliquots were collected into 1 M carbonate free NaOH for total dissolved CO_2 and H_2S analysis, respectively. The third aliquot was filtered through a 0.2 µm filter for F determination and the fourth aliquot was also filtered through a 0.2 µm filter and acidified (0.5% Suprapur HNO_3) for Na, K, Cl, Ca, Mg, Fe, Al, Si, B and SO_4 analysis. The sampling procedure is shown in Figure 2.

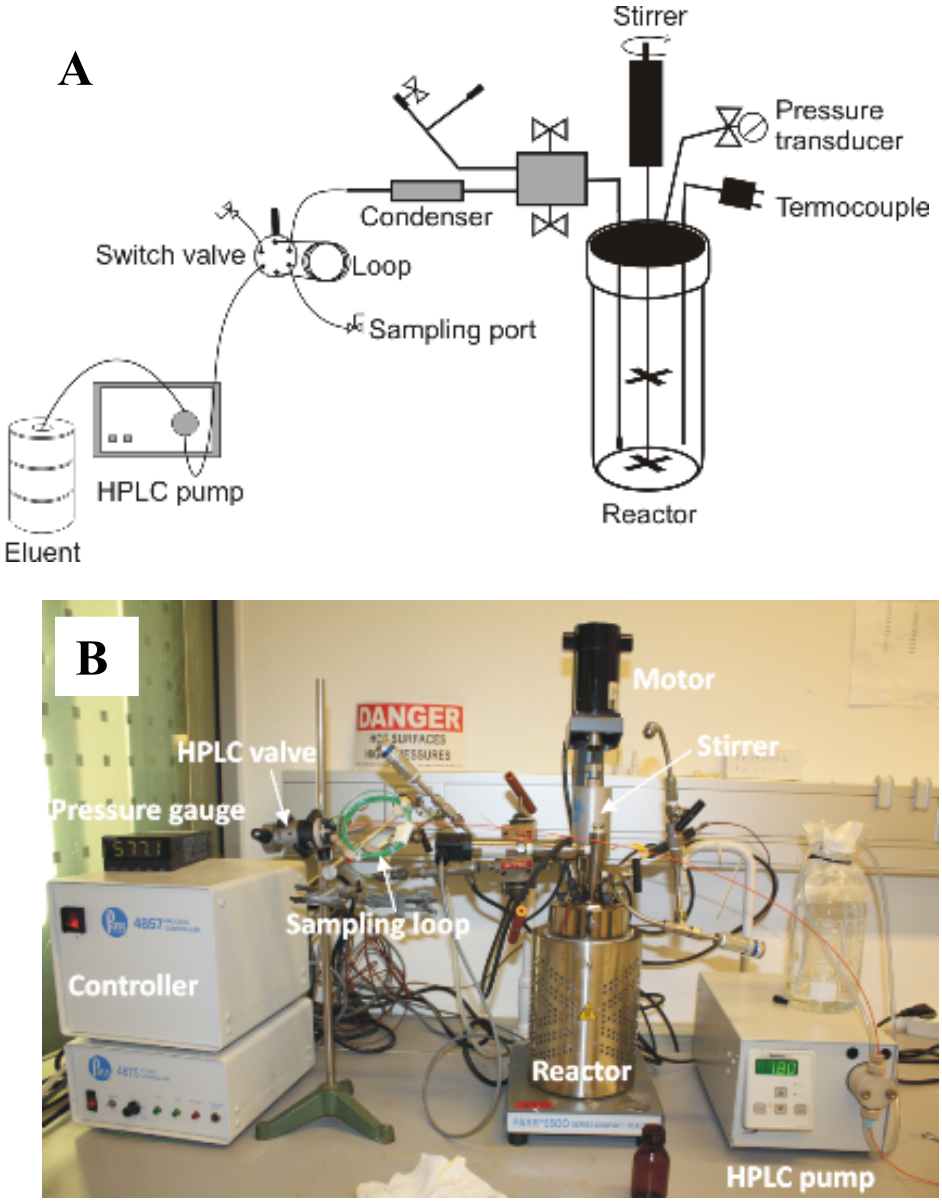

Figure 1. A) Schematic diagram of the experimental and sampling equipment used in the present study. B) Picture of the equipment.

Table 3. The initial experimental conditions.

Experiment	Material	Duration (days)	Material mass (g)	Vellankatla water (g)	Water/rock	Na_2S*9H_2O (mg)	pCO_2 (bar)
1	A75	94	40.1	379	9.5	382	2.1
2	A75	30	40.1	397	9.9	390	1.0
3	H3W	42	40.1	397	9.9	378	1.5

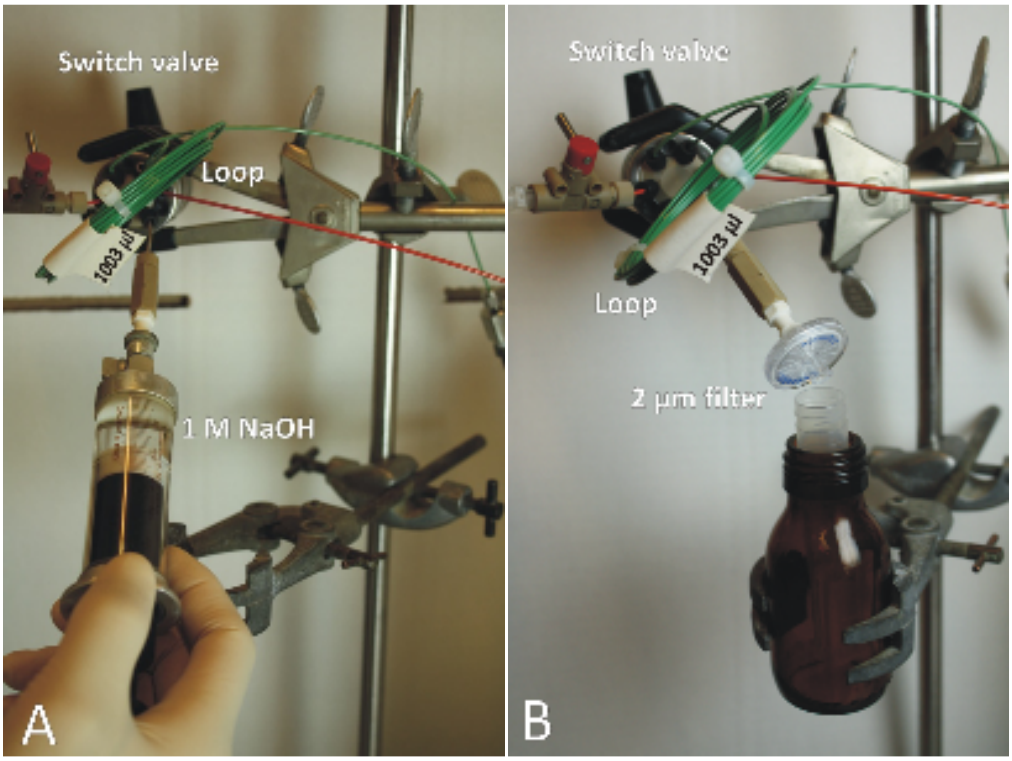

Figure 2. A) Sampling for CO_2 and H_2S determinations. B) Sampling for major elemental analysis using selective electrode and ICP analyses.

2.3 Analysis of secondary mineralogy and water composition

The major chemical composition of the water samples was analysed according to standard methods for geothermal fluids (Arnórsson et al., 2006). Total dissolved carbon (CO_2) was analysed by modified alkalinity titration and the results corrected for CO_2 in blank samples (1M NaOH). Total dissolved sulphide (H_2S) was analysed by precipitation titration using Hg-acetate and dithizone as an indicator. Dissolved F^- was analysed using a combination ion-selective electrode and major elements including Na, K, Cl, Ca, Mg, Fe, Al, Si, B and SO_4 were determined on degassed samples by ICP-AES. The analytical precision based on duplicate analysis at the 95% confidence level was <5% for CO_2 and H_2S, <3% for F^-, and <5% for Na, K, Cl, Ca, Al, Si, B and SO_4 and <7% for Mg and Fe determined on ICP-AES.

Solid samples were collected from the reaction vessel at the end of each experiment. These were oven dried at 50°C for 24 hours prior to analysis. Determination of crystalline phases was done by X-ray powder diffraction (XRD) and scanning electron microscopy (SEM). The XRD analysis were carried out using a Philips® 1050/1140 with a Cu anode and a scintillation counter PW 1964, ran at 20 mA and 40 kV with a scanning speed of 1°/2θ/min and with a Bruker D8 Focus® with a Cu anode ran at 40 mA and 40 kV with 2.4°/2θ/min scanning speed. Clay fractions were separated from a portion of the ground bulk material by a gravitational method for XRD identification. A small quantity of that material was put into a 100 ml Erlenmeyer flask and 75 ml of deionized water were added. The mixture was stirred and let stand for at least 12 hours. After that time, the supernatant liquid was taken out with a dropper and spread out periodically over a microscope slide heated by a light. This procedure was repeated until a thin layer of the clay fraction formed. XRD runs were done on untreated air died samples, samples saturated with ethylene glycol and finally samples heated 30 minutes at 400°C after saturation with ethylene glycol. For more information about the clay determination method refer to Poppe et al. (2002).

Prior to SEM analysis grains of samples were coated with gold. The SEM analyses were done using a Zeiss Supra 25® FE-SEM instrument. Qualitative analyses were further conducted using energy-dispersive X-ray spectroscopy (EDS) with an INCA Energy 300 equipment.

2.4 Geochemical modelling

Geochemical calculations were carried out with the aid of PHREEQC program (Parkhurst and Appelo, 1999) using the llnl.dat database. This included calculations of aqueous species distribution, mineral saturation state and reaction path simulations. The solution pH values were calculated based on charge balance. For buffered systems such an approach results in insignificant errors. However, the results largely depend on the analytical uncertainties, particularly the CO_2 concentration. The analytical precisions were usually <4%, and this resulted in pH uncertainties of <0.1 units which is regarded as minor for the purpose of the present study.

Reaction path modelling (e.g. Helgeson, 1968; Marini, 2006) was carried out between the starting experimental solutions (Table 2) and the silicic rocks (Table1). The geochemical reactions were studied as a function of reaction progress (ξ) at 240°C and secondary minerals and water chemistry simulated. The reaction progress may be linked to reaction time given that the reaction rates are known as well as the mineral reactive surface area. In the present study, the water was allowed to react with the silicic rocks in series of steps and saturated secondary minerals allowed to precipitate instantaneously. No kinetics were involved, however, following Marini, (2006), the calculated reaction progress may be compared with the experimental runs using a master variable like alkalinity, that may be viewed as a sum of the extend of reaction of complex incongruent reactions.

The redox state of the solutions was modelled in two ways. Firstly, it was taken to reflect the supply of Fe(II) and Fe(III) from the dissolution reaction and consumption of Fe by secondary minerals or secondly, by assuming redox equilibrium between H_2S and SO_4.

The secondary minerals considered in the calculations were those either associated with natural geothermal systems hosted by rocks of silicic composition and those observed in the experiments. A list of the minerals considered together with their dissolution reactions and equilibrium constants are listed in Table 4.

Table 4. Reactions of interest used in this study and their respective equilibrium constants at 240°C and saturation water vapour pressure (swvp).

Mineral	***Symbol***	***Formula***	***Dissolution reaction***	***log $K_{240°C}$***
Primary phases				
Askja	A75	$SiTi_{0.01}Al_{0.21}Fe_{0.06}Mn_{0.01}Mg_{0.02}Ca_{0.04}Na_{0.10}K_{0.04}O_{2.55}$	$A75 + 1.06H^+ = 0.21Al^{3+} + 0.04Ca^{2+} + 0.03Fe^{2+} + 0.03Fe^{3+} + 0.51H_2O + 0.04K^+ + 0.02Mg^{2+} + 0.01Mn^{2+} + 0.1Na^+ + SiO_2 + 0.01Ti(OH)_4$	-2.28[a]
Hekla	H3W	$SiTi_{0.002}Al_{0.233}Fe_{0.040}Mn_{0.001}Mg_{0.002}Ca_{0.032}Na_{0.134}K_{0.045}O_{2.524}$	$H3W + 1.04H^+ = 0.233Al^{3+} + 0.032Ca^{2+} + 0.028Fe^{2+} + 0.012Fe^{3+} + 0.516H_2O + 0.045K^+ + 0.002Mg^{2+} + 0.001Mn^{2+} + 0.134Na^+ + SiO_2 + 0.002Ti(OH)_4$	-2.25[a]
Secondary phases				
Quartz	Qtz	SiO_2	$qtz + 2H_2O = H_4SiO_4$	-2.16[b]
Amorphous silica	am-Si	SiO_2	$am\text{-}Si + 2H_2O = H_4SiO_4$	-1.69[b]
Boehmite	Boh	AlOOH	$bhm + 3H+ = Al^{3+} + 2H_2O$	-1.21[c]
Calcite	Cc	$CaCO_3$	$cc + H^+ = Ca^{2+} + HCO_3^-$	-1.13[d]
Fluorite	Fl	CaF_2	$fl = Ca^{2+} + 2F^-$	-11.42[c]
Anhydrite	Anh	$CaSO_4$	$anh = Ca^{2+} + SO_4^{2-}$	-8.22[d]
Analcime	Anl	$Na_{0.96}Al_{0.96}Si_{2.04}O_6{\cdot}1.02H_2O$	$anl + 4.98H_2O = 0.96Al(OH)_4^- + 2.04H_4SiO_4 + 0.96Na^+$	-9.81[d]
Wairakite	Wai	$CaAl_2Si_4O_{12}{\cdot}2H_2O$	$wai + 10H_2O = Ca^{2+} + 2Al(OH)_4^- + 4H_4SiO_4$	-22.39[d]
Montmorillonite-Na	Mont	$Na_{0.33}Mg_{0.33}Al_{1.67}Si_4O_{10}(OH)_2$	$mont + 6H^+ = 0.33Mg^{2+} + 0.33Na^+ + 1.67Al^{3+} + 2H_2O + 4H_4SiO_4$	-7.72[c]
Illite	Ill	$K_{0.6}Mg_{0.25}Al_{1.8}Al_{0.5}Si_{3.5}O_{10}(OH)_2$	$ill + 8H^+ + 2H_2O = 0.25Mg^{2+} + 0.6K^+ + 2.3Al^{3+} + 3.5H_4SiO_4$	-7.02[c]
Low-albite	Alb	$NaAlSi_3O_8$	$ab + 8H_2O = Na^+ + Al(OH)_4^- + 3H_4SiO_4$	-13.42[e]
Microcline	Mic	$KAlSi_3O_8$	$mic + 8H_2O = K^+ + Al(OH)_4^- + 3H_4SiO_4$	-14.40[e]
Pyrite	Pyr	FeS_2	$pyr + 2H^+ + H_{2(aq)} = Fe^{2+} + 2H_2S$	1.67[d]
Magnetite	Mt	Fe_3O_4	$mt + 4H_2O = Fe^{2+} + 2Fe(OH)_4^-$	-27.02[d]
Hematite	Hem	Fe_2O_3	$hem + 5H_2O = 2Fe(OH)_4^- + 2H^+$	-31.09[d]
Clinochlore	Chl	$Mg_6Si_4O_{10}(OH)_8$	$chl + 12H^+ = 2H_2O + 4H_4SiO_4 + 6Mg^{+2}$	27.48[d]
Epidote	Epi	$Ca_2Al_2FeSi_3O_{12}(OH)$	$epi + 11H_2O + H^+ = 2Ca^{2+} + Fe(OH)_4^- + 2Al(OH)_4^- + 3H_4SiO_4$	-29.84[d]
Clinozoisite	Czo	$Ca_2Al_3Si_3O_{12}(OH)$	$czo + 11H_2O + H^+ = 2Ca^{2+} + 3Al(OH)_4^- + 3H_4SiO_4$	-25.59[d]
Prehnite	Pre	$Ca_2Al_2Si_3O_{10}(OH)_2$	$pre + 8H_2O + 2H^+ = 2Ca^{2+} + 2Al(OH)_4^- + 3H_4SiO_4$	-13.89[d]

Sources: [a] This study, [b] Gunnarsson and Arnórsson (2000), [c] llnl database, [d] Stefánsson et al. (2009; 2011), [e] Arnórsson and Stefánsson (1999).

3 Results

3.1 Solution chemistry

The results of the experiments with respect to the solution composition are given in Table 5 and shown in Figure 3 to Figure 5 as a function of experimental time. For all the experiments, a pH value between 6.4 and 7.4 at 240°C was obtained (Figure 3). For a given experiment, a relatively constant pH was observed, whereas different pH values were obtained for different experimental runs. Part of this can be explained by the variable initial CO_2 concentration, but the water-rock interaction including soluble solid leaching and secondary mineralisation may also have played a role.

The relationship between elemental concentrations and experimental time is shown in Figure 4. Several trends were observed depending on the element involved. Firstly, the concentrations of CO_2, Mg, Fe and Al all decreased relatively rapidly from the initial concentrations and then levelled off after a period of >20 days to a value of ~1000 ppm, ≤0.05 ppm, ≤0.5 ppm, ≤1 ppm, respectively, yet there are some fine variations between runs. Secondly, for Na and SO_4, the concentration levels raised relatively quickly to ~2250 and ~125 ppm, respectively. Thirdly, K and B concentrations increased during the entire experimental runs whereas SiO_2 increased initially and then decreased again after ~40 days. For H_2S, F and Ca considerable differences are observed depending on the starting material.

The changes in solution chemistry upon reaction progress indicate that dissolution of silicic rocks under geothermal conditions is incongruent. The sharp decrease of elements like CO_2, Mg, Fe and Al suggest incorporation into insoluble secondary minerals whereas the much higher but still relatively uniform concentrations of Na, SO_4 and SiO_2 suggests the incorporation of these components into secondary minerals being moderately soluble. The variable behaviour of some elements like H_2S, F and Ca between samples and runs of the same sample indicates that the dissolution process probably also plays a role, with the primary phase being heterogeneous and dissolving at various rates depending on the phase involved. Chloride is not considered to enter secondary minerals (e.g. Arnórsson and Andrésdóttir, 1995).

Chloride concentrations can, therefore, be used as an indication of rock leaching as well as to qualitatively assess experimental difficulties including boiling upon sampling. In all cases the Cl concentrations rose with experimental time indicating rock leaching, however, irregular variations in concentration of up to ~10% were observed (Figure 5) this considered to indicate the true errors associated with the elemental concentrations in the experiments.

Table 5. Chemical analyses of samples from the experiments. Units are in ppm.

Sample	Days	pH_T[a]	SiO_2	B	Na	K	Ca	Mg	Fe	Al	CO_2	H_2S	SO_4	Cl	F
Askja 1875 (A75) material 94-day experiment															
1	1	6.45	658	0.12	2368	111	7.79	0.245	8.92	1.17	3491	3.19	315	3349	3.51
2	10	6.40	808	0.40	2346	236	10.9	0.162	1.67	0.48	3409	3.09	283	3467	7.96
3	20	6.62	860	0.73	2346	301	12.6	0.046	1.11	0.29	2213	3.07	195	3580	10.2
4	31	6.89	852	1.03	2180	350	14.9	0.046	0.49	0.24	747	3.34	121	3489	10.5
5	41	6.93	717	1.24	2155	379	15.0	0.038	0.31	0.21	764	3.45	122	3469	8.80
6	52	6.40	521	1.78	2156	423	15.4	0.010	0.26	0.28	1858	3.96	122	3542	6.90
7	62	6.83	496	2.30	2084	443	15.4	0.036	0.26	0.32	980	3.39	125	3420	5.37
8	73	6.72	378	3.10	2208	537	18.4	0.142	0.42	0.64	1043	3.77	135	3713	4.53
9	94	6.63	315	3.71	1787	503	14.5	0.051	0.33	1.00	872	3.34	98	3090	2.66
Askja 1875 (A75) material 30-day experiment															
1	0	7.08	379	0.08	2447	65	2.34	0.032	0.47	4.32	1630	13.0	103	3461	1.32
2	5	7.00	690	0.73	2374	171	2.93	0.044	0.19	1.64	1432	3.34	111	3506	-
3	10	6.86	702	1.14	2333	208	4.85	0.117	0.51	1.43	1635	1.41	124	3492	5.12
4	15	6.92	750	1.57	2344	233	4.84	0.062	0.15	1.06	1483	1.63	132	3520	4.82
5	20	6.86	773	2.09	2392	252	5.62	0.153	0.16	0.81	1417	1.35	142	3635	5.35
6	25	7.02	863	2.67	2527	282	6.84	0.051	0.20	1.34	1358	1.65	155	3803	5.82
7	30	7.09	792	2.98	2417	277	6.45	0.065	0.22	0.83	1261	1.70	147	3628	5.99
Hekla (H3W) material 42-day experiment															
1	0	6.99	454	0.08	2298	159	7.12	0.281	0.38	4.85	2482	2.47	146	3197	10.4
2	5	7.01	748	0.37	2326	239	3.76	0.043	0.26	2.41	2492	13.0	131	3311	-
3	10	6.91	632	0.84	2279	240	6.10	0.075	0.25	5.56	2200	19.1	129	3285	30.4
4	15	6.97	646	1.29	2383	253	4.95	0.097	0.23	4.31	1830	23.5	135	3468	31.3
5	20	7.21	596	1.58	2321	243	4.26	0.049	0.11	3.17	1319	21.7	129	3346	29.3
6	25	7.29	604	1.89	2278	233	3.29	0.026	0.06	2.46	1174	19.7	125	3269	28.6
7	31	7.39	706	2.28	2364	249	3.30	0.021	0.06	2.15	1042	20.3	130	3393	30.1
8	42	7.27	795	3.35	2518	345	7.04	0.009	0.09	0.56	813	15.0	144	3827	21.6

[a] Calculated assuming charge balance and using PHREEQC and llnl.database.

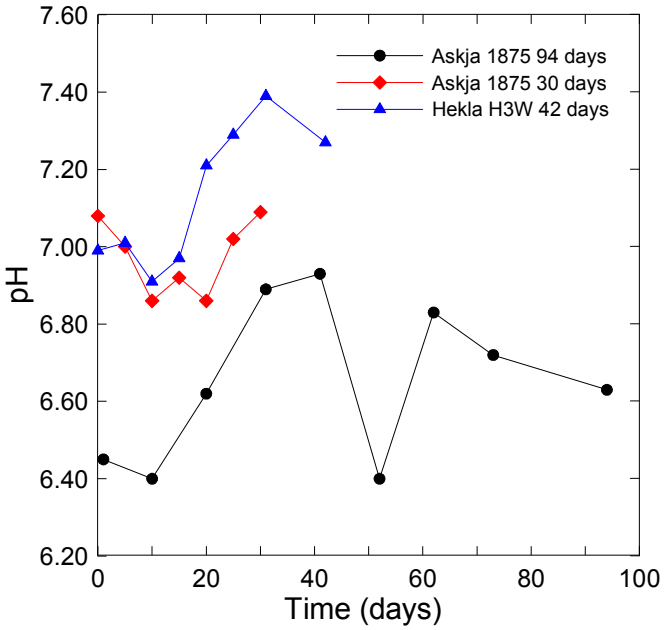

Figure 3. The relationship between solution pH at 240°C calculated based on charge balance and experimental duration for the two Askja sample runs and one Hekla sample run.

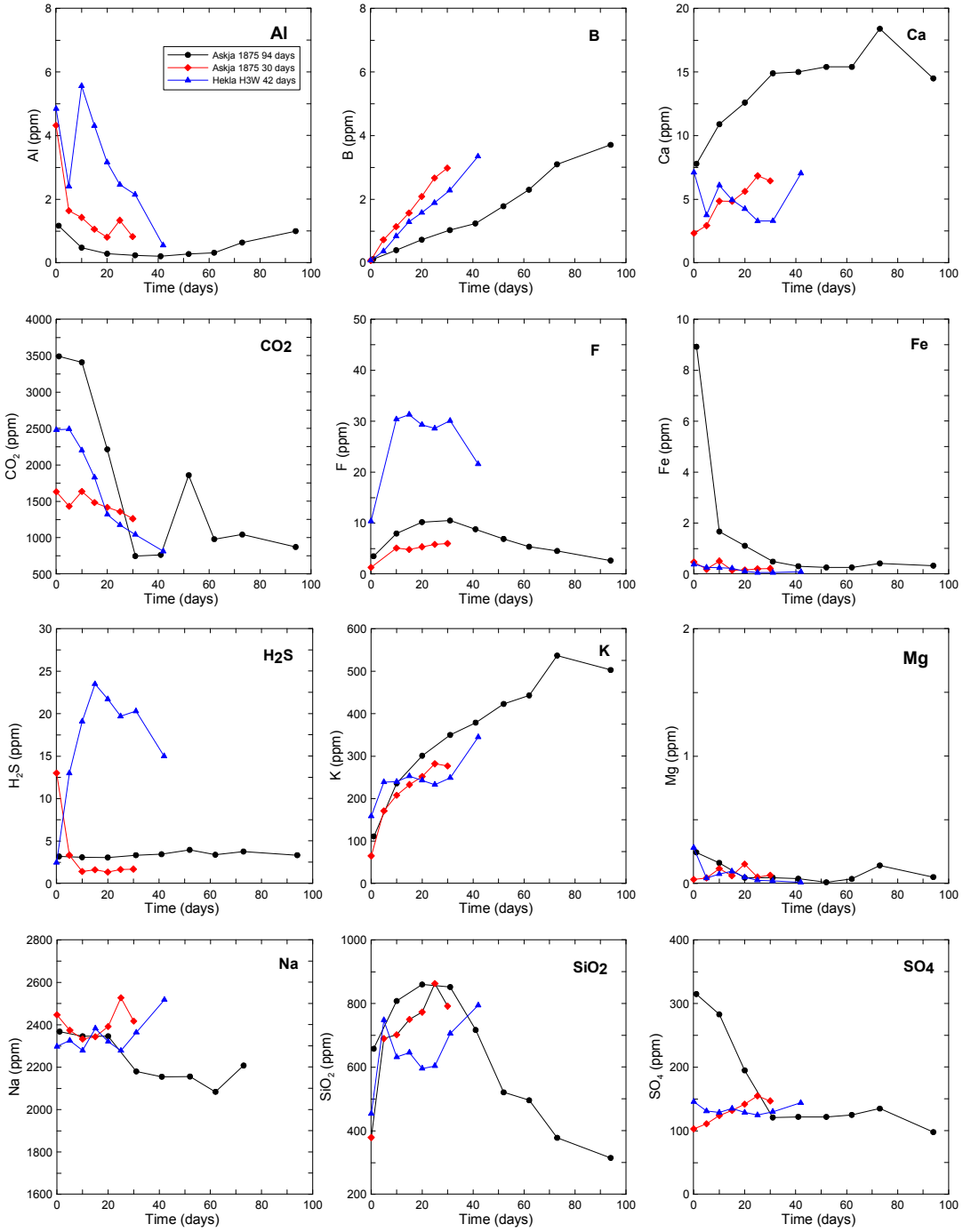

Figure 4. The relationships between solute concentration and experimental duration for the two Askja sample runs and one Hekla sample run.

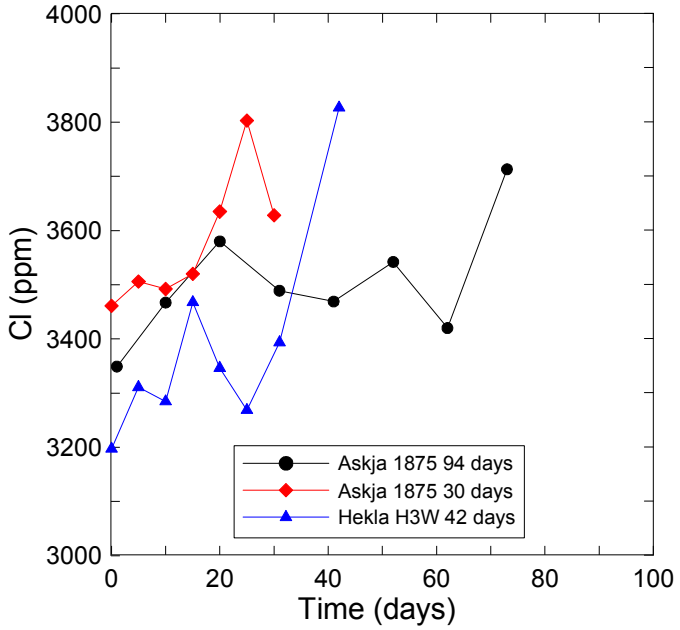

Figure 5. The relationships between dissolved Cl concentration and experimental duration for the two Askja sample runs and one Hekla sample run. Chloride is considered mobile and increased Cl concentration is considered to indicate increased rock leaching. On the other hand, irregular concentration variations are considered to reflect true sampling and analytical uncertainties.

3.2 Secondary mineralogy

The primary material and secondary minerals were studied for each experimental run using XRD and combined SEM and EDS. The secondary phases identified are listed in Table 6 and representative SEM pictures are shown in Figure 6 and Figure 7. Appendices A and B shows XRD patterns and supplementary SEM images, respectively.

Comparing unaltered and altered glass samples, it was observed that the dissolution process was localized rather than uniform and resulted in formation of dissolution pits and cracks as well as the disappearance of the sharp edges on the glass particles (Figure 6). The same pattern was observed in both Askja and Hekla samples. After 30 days of experiment, the Askja glass (A75) appeared relatively fresh and apart from showing indications of dissolved surfaces, there was very little mass of alteration products observed. On the other hand, for the Askja experiment lasting 94 days, a considerable amount of alteration product was observed with little primary glass visible within the bulk material at the end of the experiment. For the Hekla glass (H3W) considerable alteration was observed after 42 days of reaction.

The identification of secondary minerals in the experiments is non-trivial. Firstly, the quantity the secondary phases over the primary material was often little, making measurements dominated by the primary material difficult. Secondly, usually more than one mineral coexist with similar elemental composition, making accurate evaluation of mineral phases and their composition difficult. Gysi and Stefánsson, 2011) identified the clay and zeolite composition from similar experiments on basaltic glasses based on extensive electron microprobe analysis (EMPA), energy- and wave-dispersive spectrometer mapping (EDS and WDS) and mixing-models and calculated the mineral

composition, however, such a extensive mineralogical work was not undertaken in the present study. Instead, the results of the XRD, SEM and EDS were combined in order to evaluate the mineral phases of importance without identifying their exact chemical composition.

The secondary minerals identified after 42 days of reaction of the Hekla samples included quartz, anhydrite, anatase and possibly calcite. In addition, F was observed and associated with Ca suggesting fluorite formation, however, substitution of F for OH in montmorillonite cannot be ruled out as the samples were also relatively Na rich. Three populations of Al-Si minerals were identified including Na rich phase with traces of Ca, Fe and K, Fe-rich phase with traces of Na, K and Ca and Fe-K rich phase with some Na, Mg and Ca. According to XRD, analcime and illite were present as alteration products. The alteration products were, however, small and textures were difficult to recognise using the SEM but the results of the XRD and EDS are in reasonable agreement. Based on the above it is considered likely that Si-Al alteration minerals consisted of illite and/or mixed illite-smectite, analcime and possibly also wairakite, and Fe-rich chlorite, these minerals commonly associated with the geothermal alteration of silicic rocks (e.g. Lonker et al., 1990; Reyes, 1990; Harvey and Browne, 1991; Beaufort et al., 1992; Inoue et al., 2004; Mas et al., 2006).

The secondary minerals identified for the two experiments using the Askja sample included quartz, calcite and anhydrite. In addition, F-rich phase was identified in the run lasting 94 days coexisting with Ca suggesting the presence of fluorite. According to XRD analysis, three Al-Si minerals were formed including Na-montmorillonite, analcime and phillipsite. According to SEM and EDS analysis, more types of Al-Si phases were probably formed. Three compositional and textural groups were identified. The first was a Na-rich Al-Si mineral with traces of K, Ca and sometimes Fe. The phase formed irregular plates and threats on the glass surface similar to clays including montmorillonite. The second was Fe- and/or Mg-rich and contained also K, Na, and Ca suggesting a smectite and/or chlorite. These minerals showed irregular forms and sometimes platy structures. Moreover, rosettes of plates similar to those observed for chlorites were also observed. The third mineral group was Ca- and Na-rich sometimes with traces of K. The minerals formed masses or granular forms and are likely to be zeolites like analcime, wairakite and/or phillipsite. In addition, boehmite and amorphous silica were also observed, these phases most likely formed upon quenching of the experimental solutions. Based on the above it is considered that Na-montmorillonite, Fe(Mg)-rich chlorite and zeolite like analcime predominated in the Al-Si mineralogy. It is interesting that illite and/or mixed illite-smectite minerals seems to be absent in the alteration product of the Askja sample. The reason for this is not clear, however, the Askja sample contains significantly more Fe, Mg and Ca and somewhat less Na and K compared to the Hekla glass. This may have resulted in other clays like Fe-Mg chlorites and montmorillonite being stable leading to less availability of Mg for illite formation. Other causes, including mechanism of crystallisation may also have played a role.

Table 6. Summary of secondary minerals identified in the experiments.

Mineral	Formula	A75 94-day	A75 30-day	H3W 42-day	XRD	SEM
Oxides, carbonates, sulphates and fluorides						
Quartz	SiO_2	x	x	x	x	x
Calcite	$CaCO_3$	x		(x)	x	x
Anhydrite	$CaSO_4$	x		x		x
Fluorite	CaF_2	(x)	(x)	(x)		(x)
Anatase	TiO_2	(x)	(x)	(x)		(x)
Boehmite	γ-AlO(OH)		x		x	
Amorphous silica	SiO_2	x		x	x	x
Clays						
Montmorillonite	$(Na,Ca)(Al,Mg)_6(Si_4O_{10})_3(OH)_6$•nH2O	x		(x)	x	x
Illite	$(K,H_3O)(Al,Mg,Fe)_2(Si,Al)_4O_{10}[(OH)_2,(H_2O)]$			x	x	(x)
Chlorite	$(Fe,Mg)_3Fe_3AlSi_3O_{10}(OH)_8$	(x)		(x)		(x)
Zeolites						
Analcime	$NaAlSi_2O_6$•H_2O	x	x	x	x	x
Wairakite	$CaAlSi_4O_{12}$•$2H_2O$	(x)		(x)		(x)
Phillipsite	$K_2(Ca_{0.5},Na)_4[Al_6Si_{10}O_{32}]$•$12H_2O$	x			x	(x)

x = confirmed, (x) = presence inferred by chemical composition.

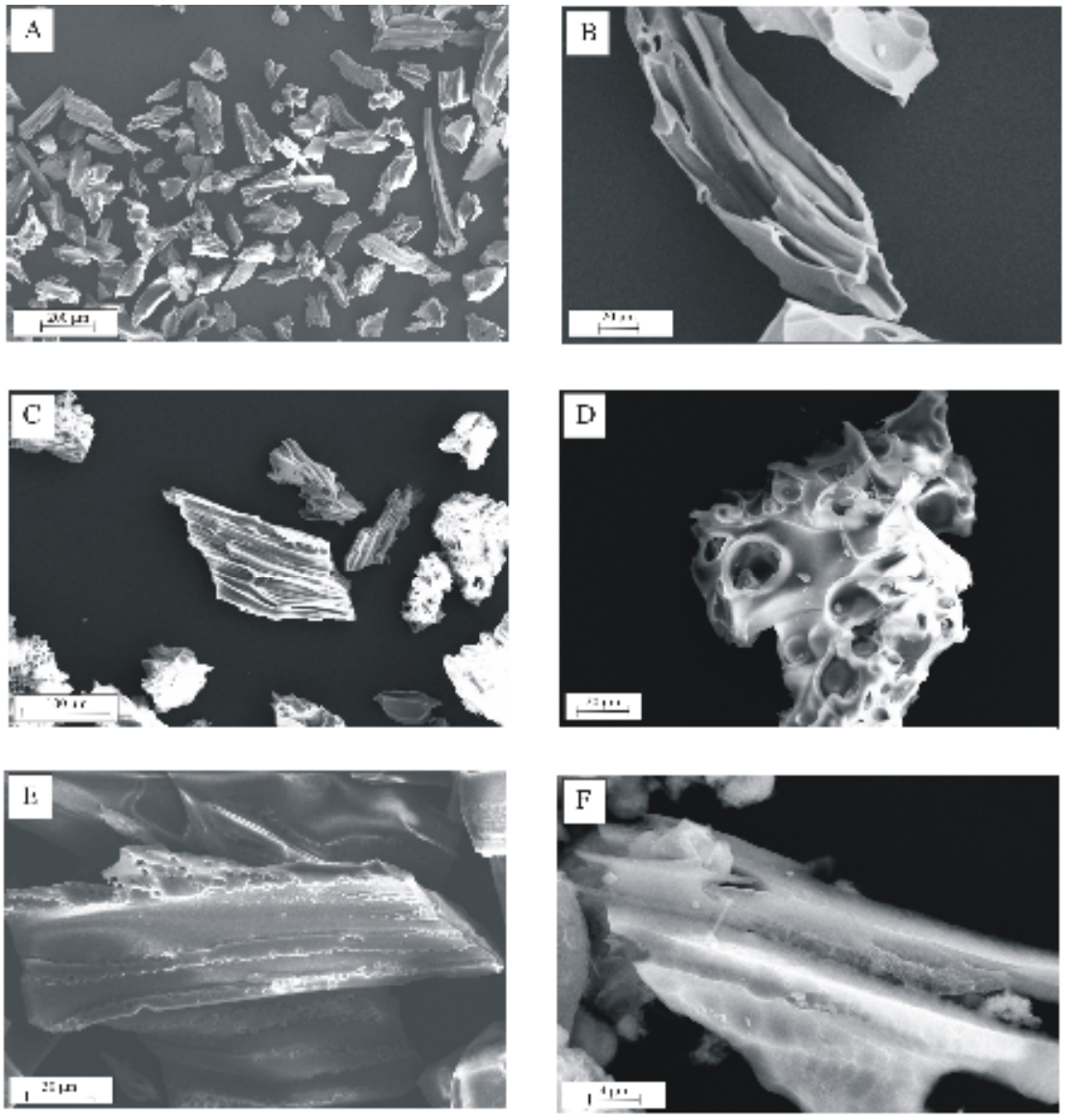

Figure 6. Scanning electron micrographs of the glasses used in the experiments. A,B) Fresh Askja 1875 (A75) material. C,D) Fresh Hekla 3W, 2900 BP (H3W) material. E) Localized dissolution or "pitting" on A75 glass after the 30-day experiment. F) Effect of dissolution over 42 days on H3W glass.

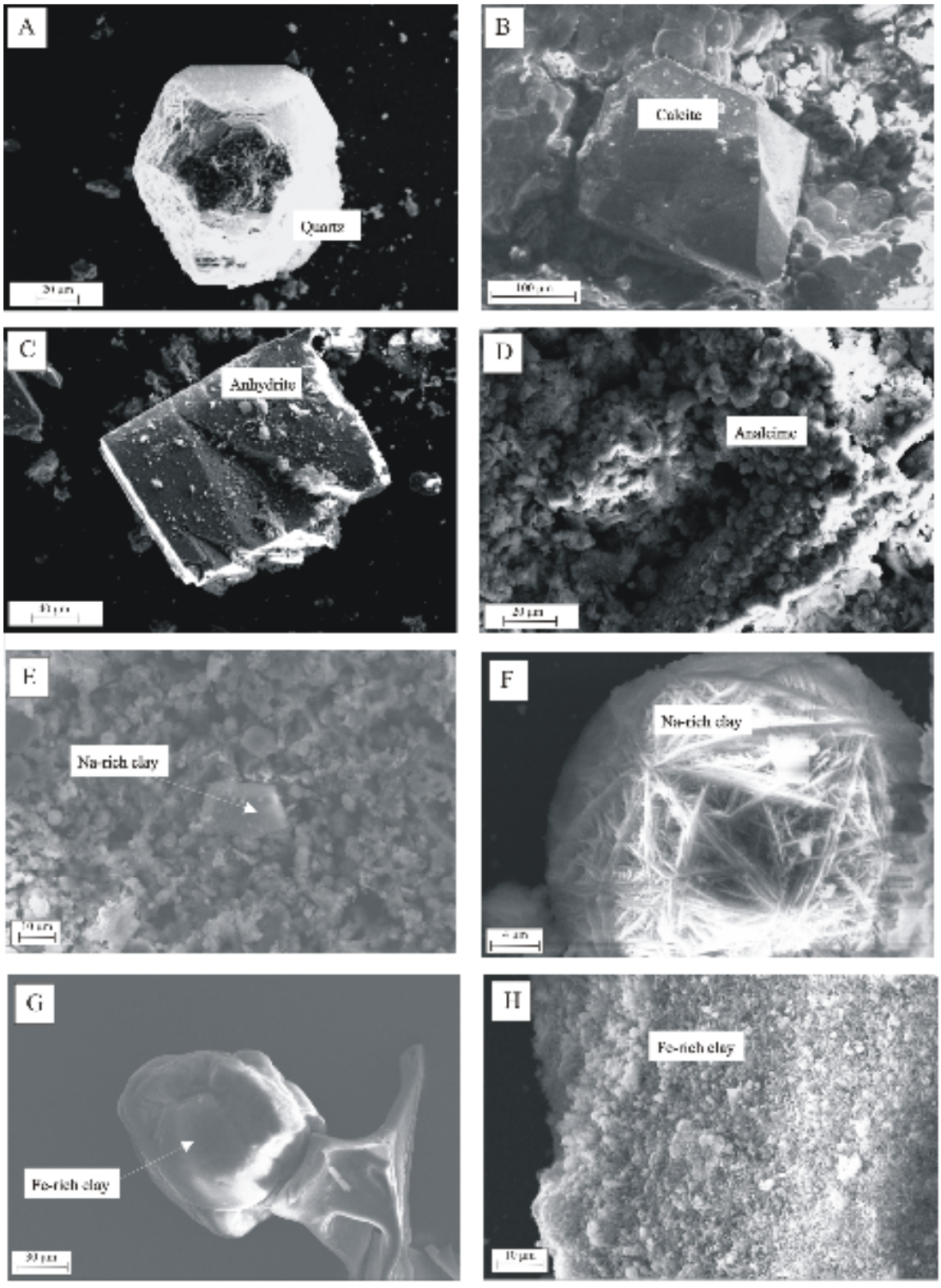

Figure 7. Scanning electron micrographs of the main alteration minerals found after the experiments. A) Quartz. B) Calcite. C) Anhydrite. D) Zeolite, most probably analcime. E, F) Na-rich clays, probably montmorillonites. G) Fe-rich clay, probably chlorite. H) Fe rich-clay with K, mixed illite-smectite.

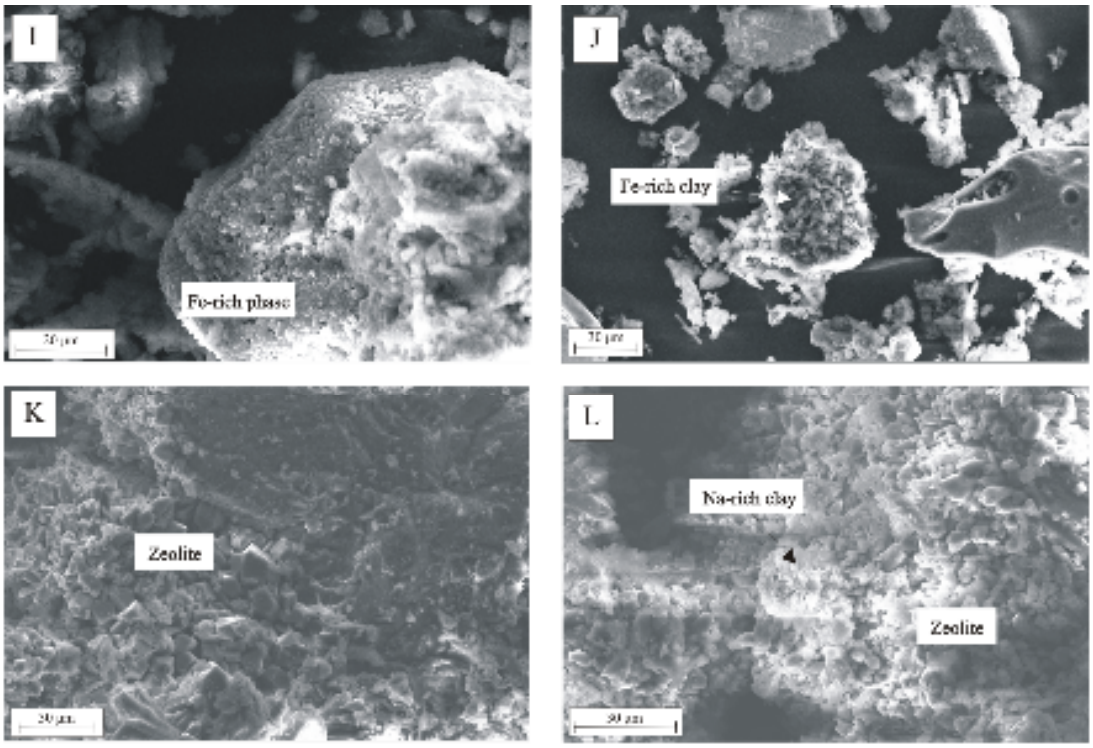

Figure 7 cont. I) Fe-Si-O rich phase. J) Fe-rich clay, smectite/chlorite. K) Zeolite, probably analcime. L) Na-rich clay next to a zeolite (analcime, wairakite or phillipsite).

4 Water-silicic rock interaction under geothermal conditions

4.1 Elemental mobility and mineral saturation

The relative mobility of a particular element either in the liquid or in the solid phase is a very useful indicator to evaluate if a particular element is enriched in the water phase or the solid phase. With respect to the water samples, the relative mobility (RM_i) was calculated based on

$$RM_i = \frac{([i]/[B])_{water\ sample}}{([i]/[B])_{rock}}$$

where RM_i is the concentration ratio of the *i-th* element in a particular water or alteration sample and in unaltered rock (Table1) relative to the reference element. Following Arnórsson and Andrésdóttir (1995), B was chosen as the reference element. It shows apparent high mobility compared to most other major elements under the pH range of the present study.

The values for B, Cl and F in Askja A75 and Hekla H3W glasses were assumed to be identical and estimated from elemental correlations. The concentration of B in Icelandic obsidian from Hrafntinnusker is 22 ppm whereas for rhyolitic glasses of Long Valley, California, concentrations up to 116 ppm have been reported (Smith and Simon, 2004; Rózsa et al., 2006). Based on B concentration range in rhyolitic glasses, a median value of 47 ppm was selected. Based on linear correlation between K_2O and Cl in Icelandic basalts, the K_2O content Askja glass would imply a Cl concentration of 22000 ppm (Sigvaldason and Óskarsson, 1976), which is most likely an overestimation of the true value. On the other hand, Icelandic rhyolites contain on average 1250 ppm Cl (Gunnarsson et al., 1998). Selecting median values for Askja glass of 7000 ppm Cl and 47 B ppm and assuming Cl and B to be conservative, resulted in a value based on mass balance of 0.42 and 0.34 moles of glass reacted at the end of the 94-day experiment, considered to be reasonable. In addition, F concentration for Askja glass was assumed to be 2080 ppm, according to the values reported by Gunnarsson et al. (1998).

The results of the elemental mobilities relative to B are shown in Figure 7. Assuming B to be mobile, the increased B concentrations with time are considered to represent progressive rock dissolution. Aluminium was initially released stoichiometrically but upon reaction progress it became immobile. Calcium was observed to be less mobile than B and reached a constant value after some time, higher for the Askja 94-day experiment than for the other two runs. The reason for this is not clear. Chloride was observed to be more mobile than B. Fluoride was observed to dissolve stoichiometrically but showed much lower mobility in later stages in the Askja runs. Both mobility of this anion and quantities released from the rock were particularly higher in Hekla than in A75 glass. At the beginning of the experiments, Na behaved as a mobile element but as reaction

progress advanced, the concentration started to decrease suggesting quantitative removal from solution. Potassium was the element that presented the highest mobility of the major elements throughout the experiments. It only became immobile in the final stages of Askja 30-day and Hekla experiments. Elements like Fe and particularly Mg were the least mobiles. Solutions were rapidly depleted from their initial concentrations. Important SiO_2 amounts (400-800 ppm) were leached from the rock at the initial stages of the experiments and this element was incorporated into solutions in a stoichiometric manner. Later on, its mobility decreased and this effect was very well observed in Askja 94-day experiment.

Another useful measure for studying secondary mineral formation is the mineral saturation state. The saturation index of secondary and primary minerals is defined by

$$SI = log\,(Q_r/K)$$

where the K is the equilibrium solubility constant for a particular mineral reaction and Q_r is the reaction quotient given by

$$Q_r = \prod a_i^{v_i}$$

where $a_i^{v_i}$ is the activity of the *i-th* mineral or aqueous species and v_i is its reaction stochiometry, positive for products and negative for reactants. When mineral dissolution or precipitation reactions are written with the minerals to the left (reactant), negative saturation indices indicate undersaturation and the respective mineral is unstable or has the tendency to dissolve if it is present in the system. Zero and positive saturation indices indicate saturation and supersaturation, respectively, and that the minerals are stable and have the potential of precipitating.

The secondary mineral saturation was studied with respect to the experimental solutions as a function of time. The secondary minerals considered were those observed in the experiments as well as those commonly associated with geothermal alteration at ~240°C. The secondary minerals, their respective dissolution/precipitation reactions and the equilibrium solubility constants are summarised in Table 4.

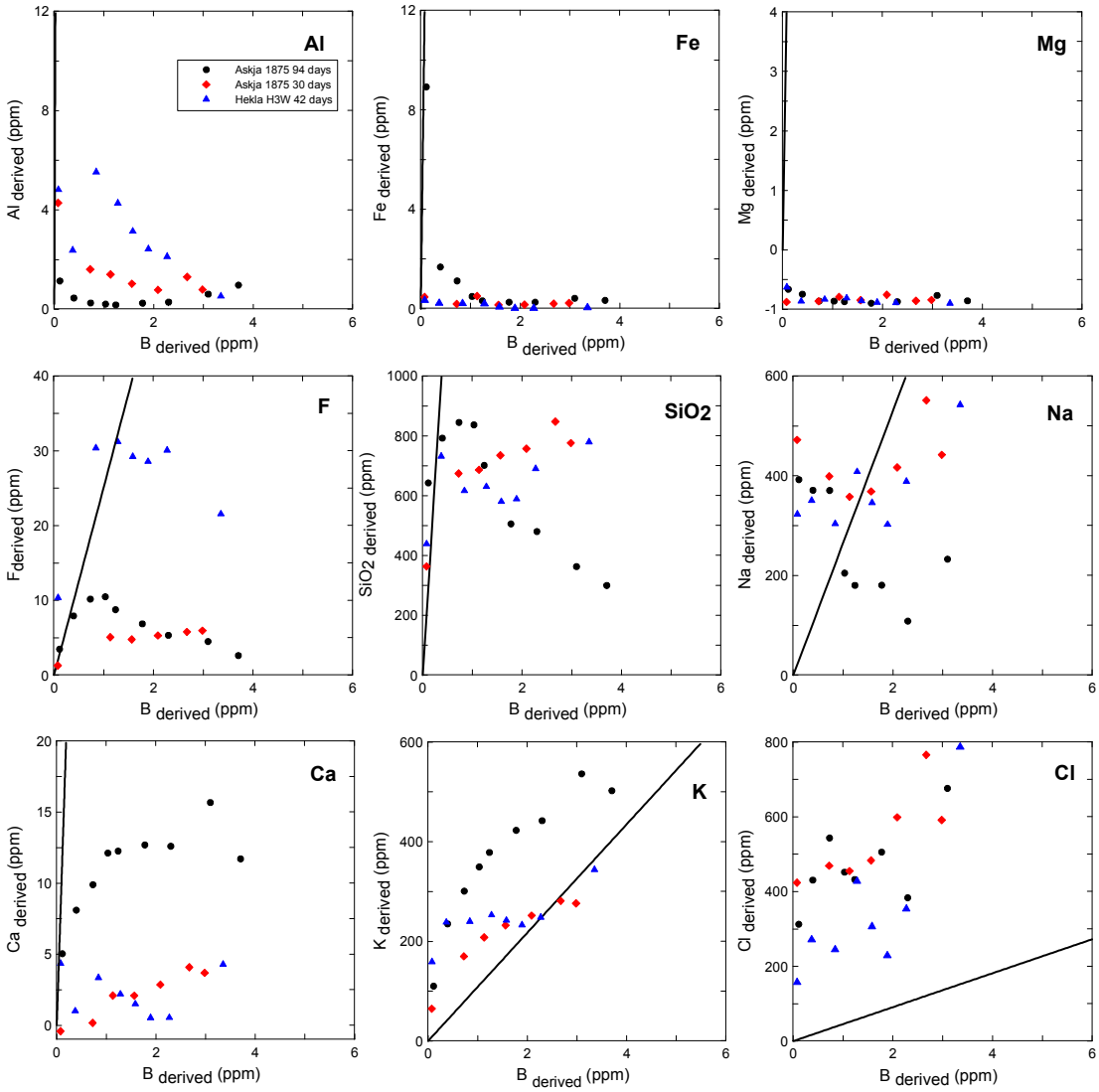

Figure 7. The mobility of major elements in the water samples relative to B. The symbols delineate the experimental concentrations whereas the lines the respective rock rations. Water samples plot above or onto the line are considered to represent mobile behaviour whereas water samples plotted below (to the right) are considered to indicate apparent lower mobility than B and incorporation of the elements into secondary minerals. The water sample concentrations were corrected for initial composition, i.e. $[i]_{derived} = [i]_{measured} - [i]_{initial}$

The saturation state with respect to the common secondary minerals observed is shown in Figure 8, Appendices C and D. Most of the minerals observed were found to be close to saturation including analcime, calcite, Na-montmorillonite, illite and chlorite. On the other hand, quartz was observed to be supersaturated for the first weeks eventually reaching saturation afterwards. Anhydrite, amorphous silica and boehmite were on the other hand slightly undersatured in all cases. This may be because these minerals were not present under the experimental conditions and were rather formed upon quenching at the end of the runs. Other minerals that are commonly associated with geothermal alteration at ~240°C including pyrite, prehnite and feldspars were observed to be supersaturated. Epidote and iron oxides were undersaturated throughout the runs. Many of these minerals contain redox sensitive elements like sulphur and iron. For thermodynamic aqueous speciation calculations, a single redox state needs to be selected. This may, however, not have been attained (Stefánsson and Arnórsson, 2002; Stefánsson et al., 2005). The redox potential of a given water sample is one of the main sources of error and uncertainties in the calculation of mineral saturation states in acid surface geothermal waters. The redox pair chosen for the calculations was the S(-II)/S(VI) ratio. However, the value probably does not always indicate the true ratio and other redox reactions may not be in equilibrium with the S(-II)/S(VI) ratio like Fe(II)/Fe(III).

In summary, Al, Fe and Mg showed a reduced mobility during all the experiments suggesting that these elements were quantitatively incorporated into secondary minerals in zeolites like analcime, clays like montmorillonite, illite and chlorite and possibly other Al-Si containing minerals. Sodium, Ca and Si all showed reduced mobility upon reaction progress. Silica is considered to have entered into various Al-Si minerals and quartz whereas Na and Ca were incorporated into minerals like analcime, montmorillonite, calcite and anhydrite. It is further interesting to note that K was observed to be relatively mobile during the experiments compared to most other elements. However, despite K-bearing minerals like microcline and illite were observed to be saturated or supersaturated potentially removing K from solution, this was not seems to be the case quantitatively.

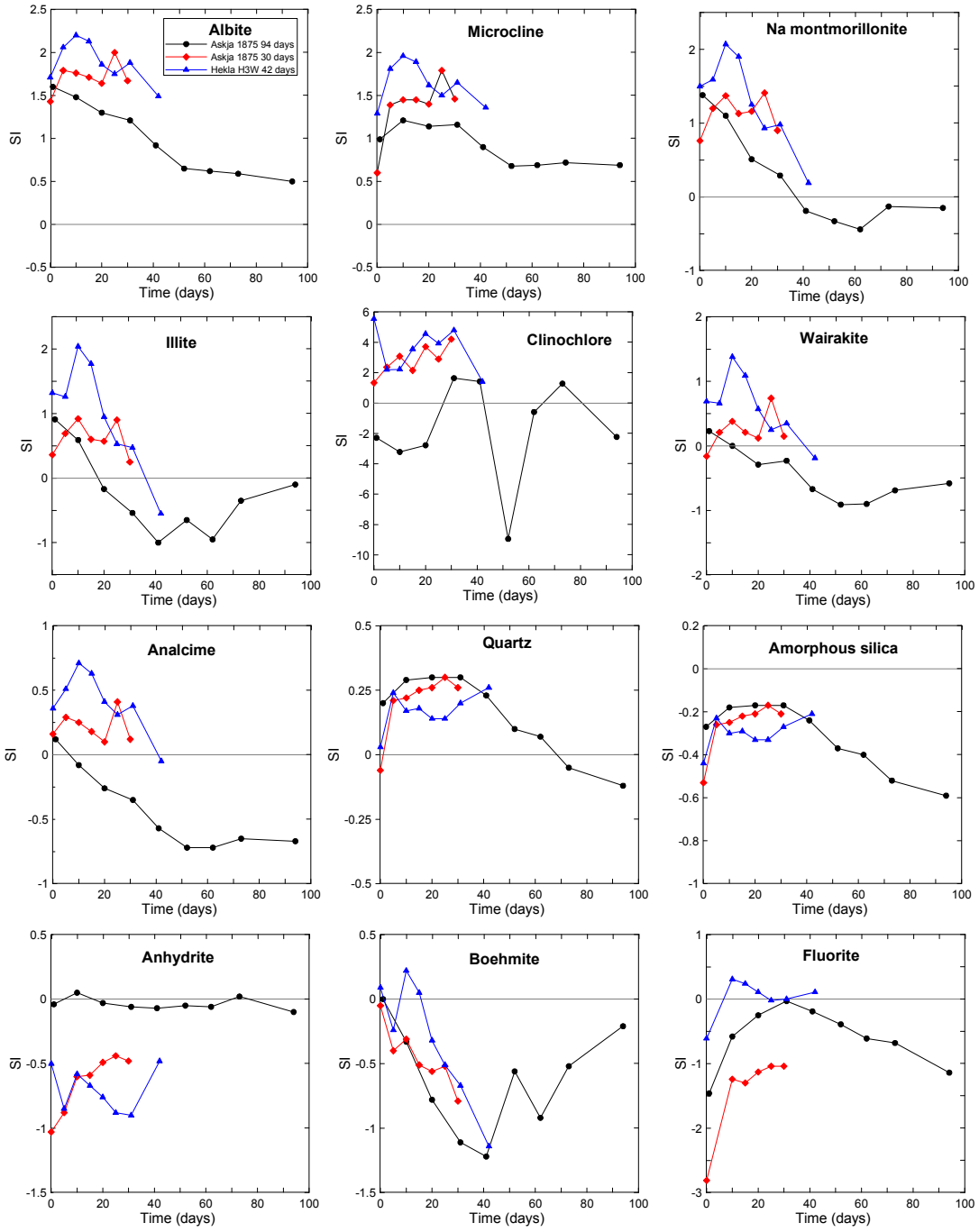

Figure 8. The saturation indices of selected secondary minerals.

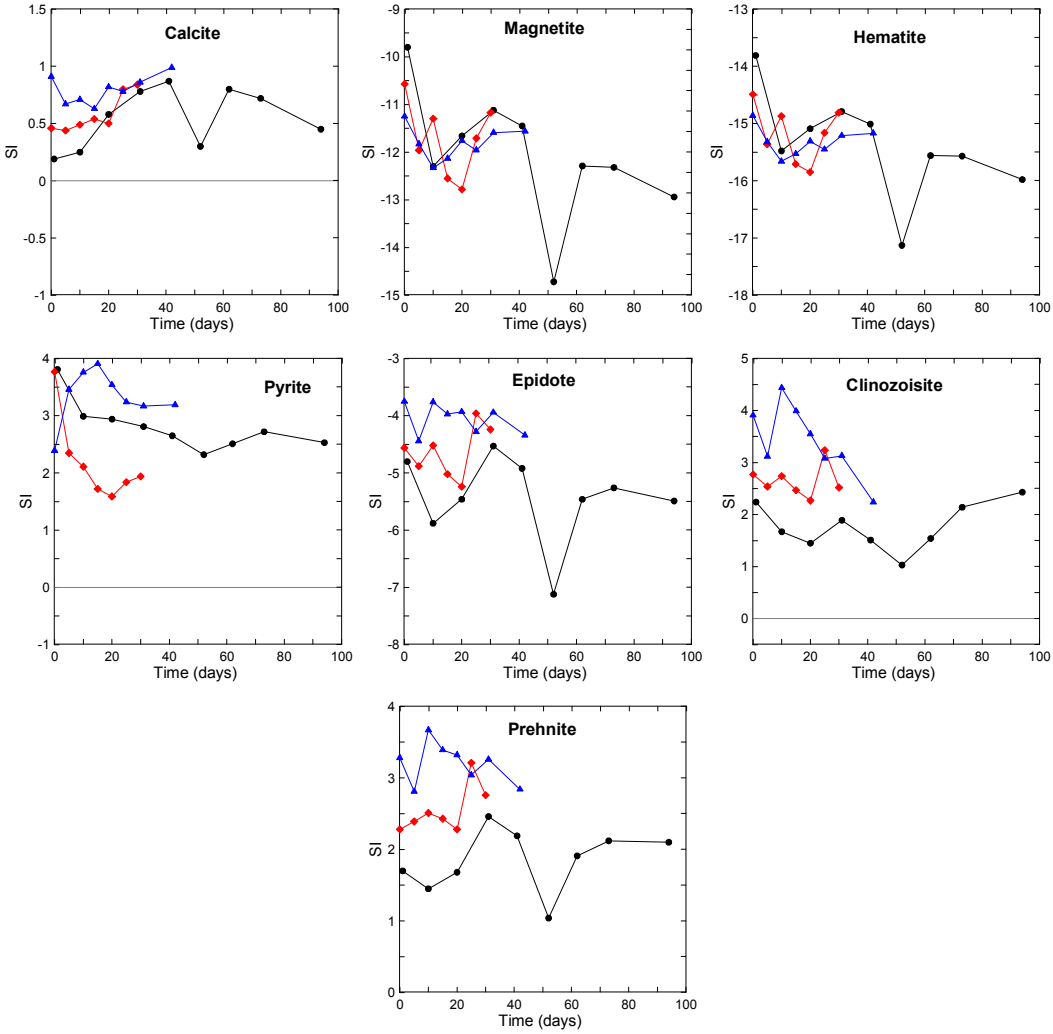

Figure 9 cont. The saturation indices of selected secondary minerals.

4.2 Reaction path simulations and comparison with experimental observations

To get further insight into the water-rock interaction and the effect of extent of reaction, reaction path simulations were conducted. In addition, comparison with the experimental results may give additional information on the key processes of water-silicic rock interaction, including dissolution and precipitation kinetics. In the models, several moles of glass were dissolved in given number of steps in a solution similar to the experimental starting solutions and saturated minerals allowed to precipitate instantaneously.

The model results with respect to the water chemistry are compared with the experimental data in Figure 9. Following Marini (2006), the reaction progress is expressed in terms of alkalinity. The alternative definition of alkalinity implies that for every cation that is removed from the solution, a proton should be added in order to maintain a charge balance. This variable may be viewed as an average indicator of the degree of water-rock interaction, however, it may not always be the case especially if the alkalinity is dominated by dissolved CO_2 that is being mineralised resulting in decreased alkalinity with increased

reaction progress. Because of this, pH has also been used as an indicator of extend of reaction (Gysi and Stefánsson, 2011).

The modelled pH values compared reasonable well with those measured experimentally. However, a small yet significant systematic difference was observed suggesting that the balance of proton consumption and release by primary and secondary phases, that is largely mass dependent, is somewhat systematically offset. The calculations, however, are also very dependent on the CO_2 concentration that in turn was somewhat overestimated in the geochemical simulations compared to the experimental results, this resulting in lower pH values. For Si, Na and K, the experimentally determined concentrations were all greater than the modelled values. However, upon experimental reaction time both Si and K approached the values predicted by the models which are based on the saturation of quartz and K-containing clays. This situation points towards that kinetics may play an important role, at least initially, in nucleation and growth of Si, K and possibly also Na bearing phases. This is consistent with low-temperature observations at <100°C (e.g. Gysi and Stefánsson, 2011) but has not been clearly observed in geothermal conditions before to our best knowledge.

The modelling of Ca, Fe and Mg chemistry as well as the resulting pH was observed to be very dependent on the composition of the primary and secondary phases. The Askja sample contained significantly higher Mg concentrations than the Hekla ones. This resulted in Mg being the mass dependent element for Mg-Fe secondary minerals rather than Fe. Consequently, Fe concentrations were much higher in the Hekla modelling runs, resulting in more Ca-Fe secondary mineral formation and Ca depletion compared to the Askja modelling runs. Fixing Fe by addition of Fe-bearing oxides resulted, however, in water pH values <4, which is considered unrealistic. For the Askja runs, Fe was observed to be the mass depleted element, resulting in higher mobility of Ca for calcite and Ca-rich clays, zeolites and possibly epidote and prehnite mineralisation. Nevertheless, for both Ca and SO_4, lower concentrations were modelled compared to those experimentally determined. This may suggest an additional source of $CaSO_4$, in fact, introduction of small quantities of anhydrite to the starting material resulted in a better fit. This suggest that either volcanic materials, like Askja and Hekla, may contain some trace amounts of salts including $CaSO_4$, that affect the water chemistry during initial stages of water-rock interaction. Also, based on mass balance calculations it is clear that most of the H_2S got oxidised to SO_4 during the first hours of the experiments this probably explaining the excess SO_4 concentrations.

The sequences of mineral alteration according to the water-rock modelling of Askja and Hekla samples are shown in Figure 10. The results indicate that the appearance of various minerals in a closed system is initially a function of reaction progress. A similar overall pattern was obtained for both Hekla and Askja samples. Quartz, clays, zeolites and pyrite formed initially and were among the major secondary minerals together with calcite later on. Secondary minerals commonly associated with mafic rock alteration like feldspars, epidote, chlorite, magnetite and hematite were also formed during later stages, but in most cases their mass was limited at low to moderate reaction progress.

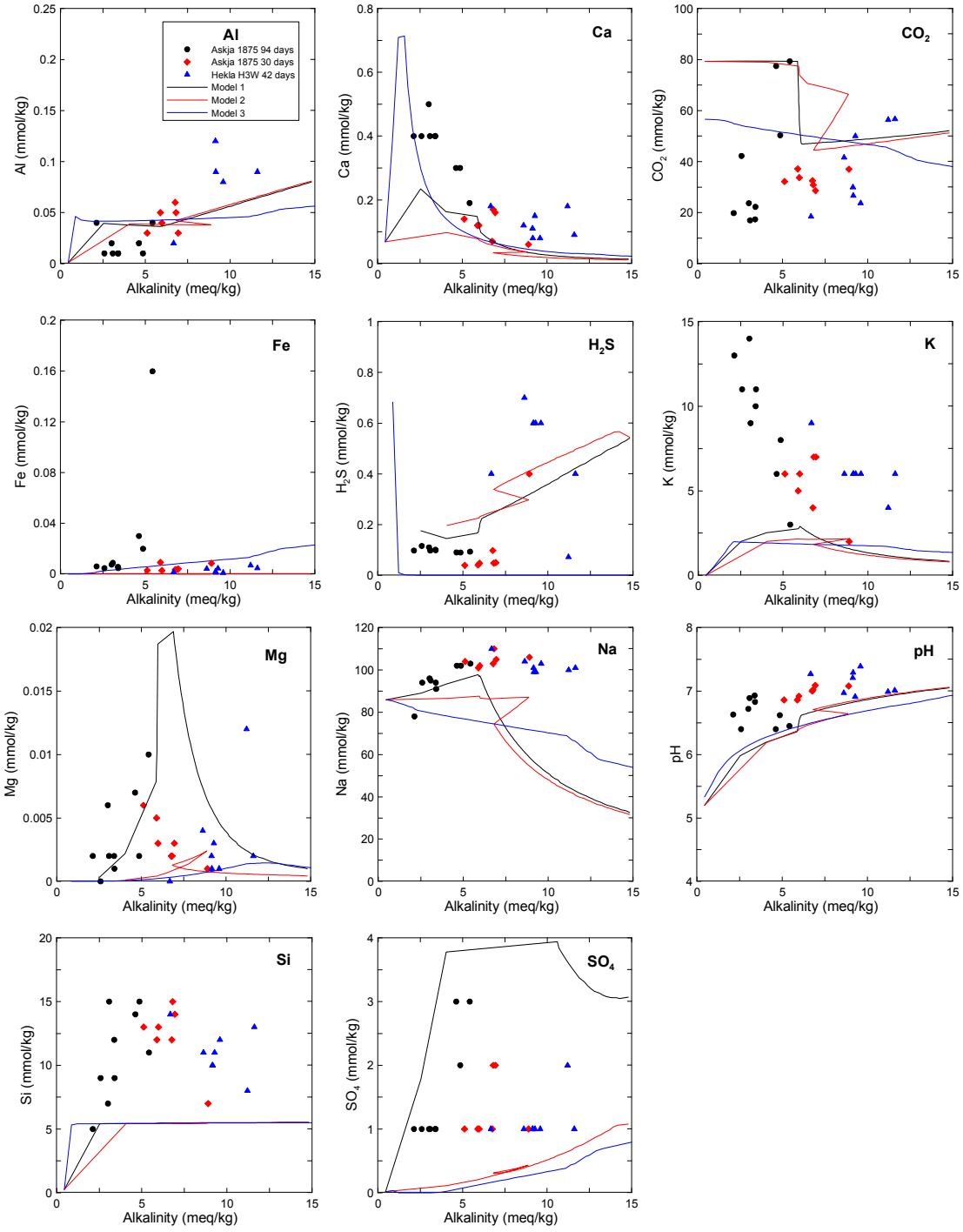

Figure 9. Comparison between experimental results and geochemical model simulations. Model I: Askja 1875 with Vellankatla starting solution. Model II: Askja 1875 with Vellankatla starting solution and traces of anhydrite ($CaSO_4$) (0.1% of total solid mass). Model III: Hekla H3W with Vellankatla starting solution.

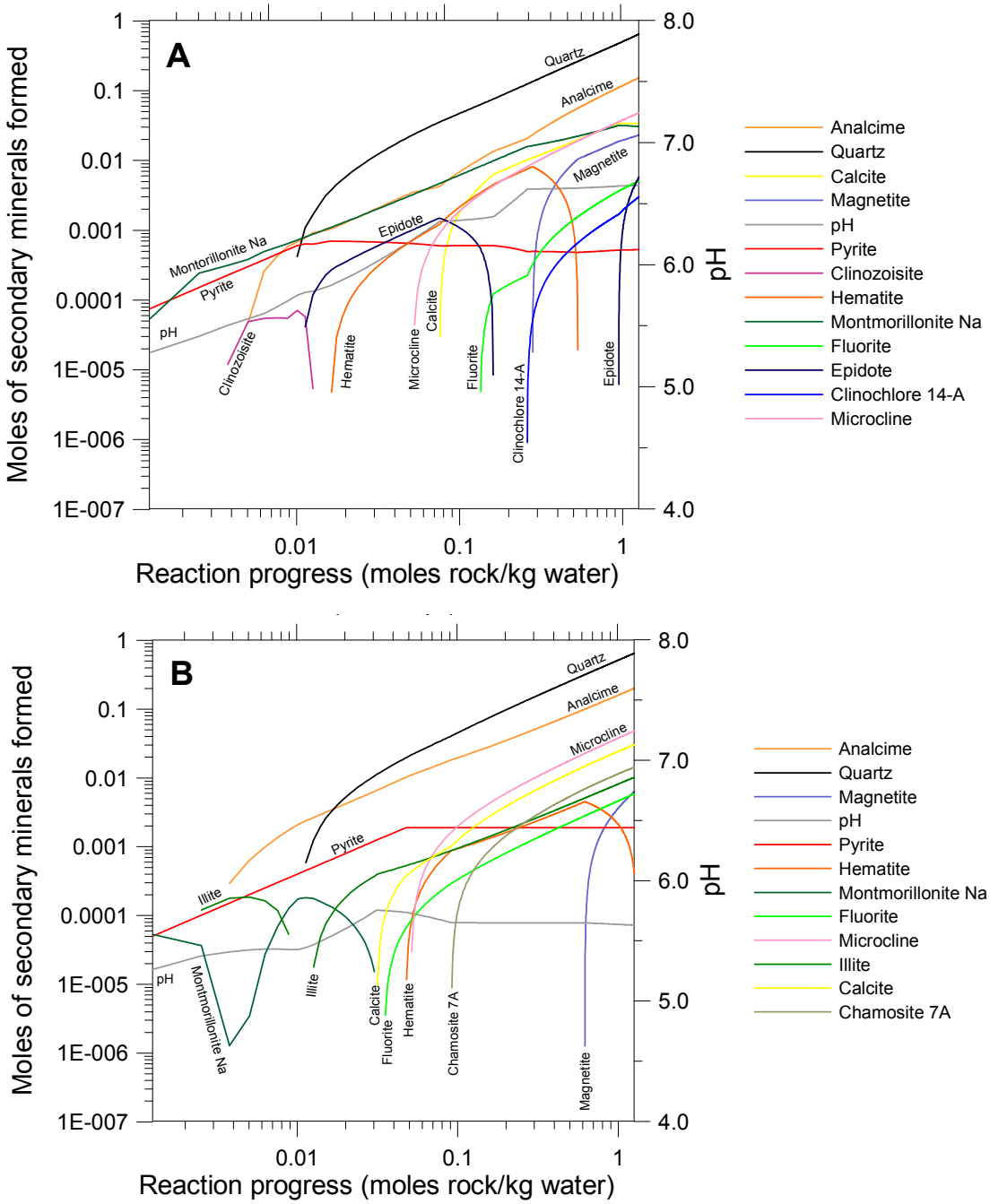

Figure 10. The results of the reaction path modelling with respect to secondary mineralogy. In the models, 1 mole of glass (~100 g) was dissolved in 1 kg of the starting solution. A) Askja 1875 sample. B) Hekla H3W sample. The results show that initially the secondary mineralogy is very dependent on reaction progress but upon extensive reaction (>0.1-1 mole glass) the system reaches a balance with minerals including quartz, zeolites (like analcime), clays (illite, montmorillonite and chlorite) and alkali feldspars.

The exact composition of the clays was also found to be dependent on the primary glass composition, Na-montmorillonite predominated in the calculations for the Askja sample whereas illite was more important for the calculations involving the Hekla sample. This is consistent with observations of Na-montmorillonite being important alteration mineral in the experiments involving Askja whereas illite was more important associated with the Hekla samples.

Summarising, the results of the reaction path simulations are in reasonable good agreement with the experimental results. Comparison show that precipitation kinetics may be of importance for some elements like Si, K and Na whereas the exact Mg, Fe and Ca composition of the primary material plays a significant role in the mass and composition of secondary Ca, Mg and Fe containing aluminium silicates and oxides. The results between the Askja and Hekla samples also show that fine compositional variations of the major ions including K, Fe, Ca and Mg have large influences on the predominant clay composition. For the Askja model, montmorillonite and chlorite predominated whereas for the Hekla model, illite was the most important clay with Fe-rich chlorite upon reaction progress, consistent with the mineralogical observations.

4.3 Model limitations

There are some considerable uncertainties associated with the model simulations that may affect the results to some degree as well as the conclusions drawn from the comparison of the geochemical models with the experimental results.

The results and comparison of the experiments and modelling suggest that the dissolution of the primary phase may not be stoichiometric with respect to all elements like F and Cl and possibly also SO_4. In fact, traces of high-albite and magnetite were observed in the Askja sample whereas high-albite was observed in the Hekla sample. The existence of other phases dissolving rather than just the glass in question, adds another variable to the systems. Moreover, comparison of the models to the experimental results suggest possible traces of soluble salts like CaF_2 and even $CaSO_4$ though the excess of SO_4 in the experiments is primarily considered to be due to H_2S oxidation.

Another problem of the geochemical model calculations is related to mineral dissolution and precipitation kinetics. As mentioned previously, the primary phase was assumed to dissolved stoichiometrically and secondary phases to precipitate instantaneously upon saturation. Taken into account only dissolution kinetics would not have affected the results, however, for a given surface area the results and mass transfer might have been linked to reaction time. The addition of dissolution kinetics as well as precipitation and crystal growth kinetics may affect the results. Firstly, if secondary mineral formation kinetics is variable, this may indeed affect the relative mass proportions formed as well as inhibit formation of some secondary phases. Based on the experimental observations, this is indeed considered to be the case for some elements like Si, K and maybe also Na. Secondly, if the dissolution kinetics is faster than the secondary mineral formation kinetics for a given element, this may result in an increase of the elemental concentration in solution above equilibrium solubility. This was observed for Si, K, Ca and Na compared to the models and secondary minerals observed.

The incorporation of both dissolution and precipitation kinetics poses one of the major challenges today for reaction modelling, as data are almost completely missing with respect to secondary mineral formation kinetics, on homogeneous polymerisation, nucleation and on crystal growth (Marini, 2006). However, all this problems do not underscore the value of reaction path modelling as a powerful tool to understand and

predict events in the complexity of the systems in terms of variables and processes when it is feed with satisfactory experimental data, but the results have to be treated with great care and viewed in terms of qualitative indicators rather than quantitative ones.

4.4 The effect of extent of reaction in closed multiphase systems and its application to geothermal geochemistry

The findings of the geochemical model calculations and the comparison with experimental results on silicic rock alteration and water chemistry at 240°C raised some important questions on the role of initial fluid composition and extent of reaction on the alteration process under geothermal conditions. Comparison of the models with the experimental results suggests that the alteration process and water chemistry is largely controlled at the early stages of alteration by the extent of reaction, fine variations in Fe, Mg and Ca content of the silicic rocks as well as precipitation and crystal growth reaction kinetics with respect to Si, K, Na and Ca. However, upon extensive rock alteration (ξ >1 moles of rock per kg of solution), the system develops to a balanced state of a given mineral assemblage of quartz, albite, K-feldspar, chlorite, Fe-epidote, illite, calcite and pyrite that are commonly associated with geothermal alteration of rhyolites and andesites (e.g. Browne, 1978; Reyes, 1990; Hedenquist et al., 1998).

One of the primary implications of the results has to do with the application of alteration mineralogy and water chemistry for estimating geothermometry temperatures. The initial rise of Si in the experiments followed by a decrease after ~40 days and eventually reaching quartz equilibrium solubility after ~60 days is reflected in the calculated quartz geothermometry temperatures (Fournier, 1977; Fournier and Potter, 1982; Arnórsson et al., 1998) with too high values of >300°C until after 40 days of reaction (Figure 11A). With respect to the Na/K geothermometry temperatures (Truesdell, 1976; Fournier and Potter, 1979; Tonani, 1980; Nieva and Nieva, 1987; Giggenbach et al., 1988; Arnórsson et al., 1998) a steady increase was observed from ~150°C at the beginning to >300°C at the end for the Askja run (Figure 11B). This is considered to be linked to the increase of K with experimental time throughout the experiment. Other cation geothermometers like Na-K-Ca (Fournier and Truesdell, 1973), Na/Ca (Tonani, 1980), K/Mg (Fournier, 1991) and K/Ca (Tonani, 1980) were evaluated (Figure 11C). The only geothermometer that gave reasonable values around 240°C was the K/Ca geothermometer. Considering that K increased steadily with experimental time and was not controlled by the formation of secondary K-bearing phases and also that Ca increased throughout the experiment, the most likely explanation to that fit is that they both augmented in a relatively constant molar ratios.

4.5 A conceptual model of water-silicic rock interaction at 240°C as a function of extent of reaction

The dissolution of silicic rocks and formation of secondary minerals and dissolved solutes may be viewed as a titration process with the primary phase being the base and the water with its dissolved acids (mainly CO_2+H_2S) the acid. At a particular stage, there is a balance in the system between the release of elements (degree of dissolution) from the primary

phase, acid supply and consumption of acids and mass and composition of secondary minerals formed.

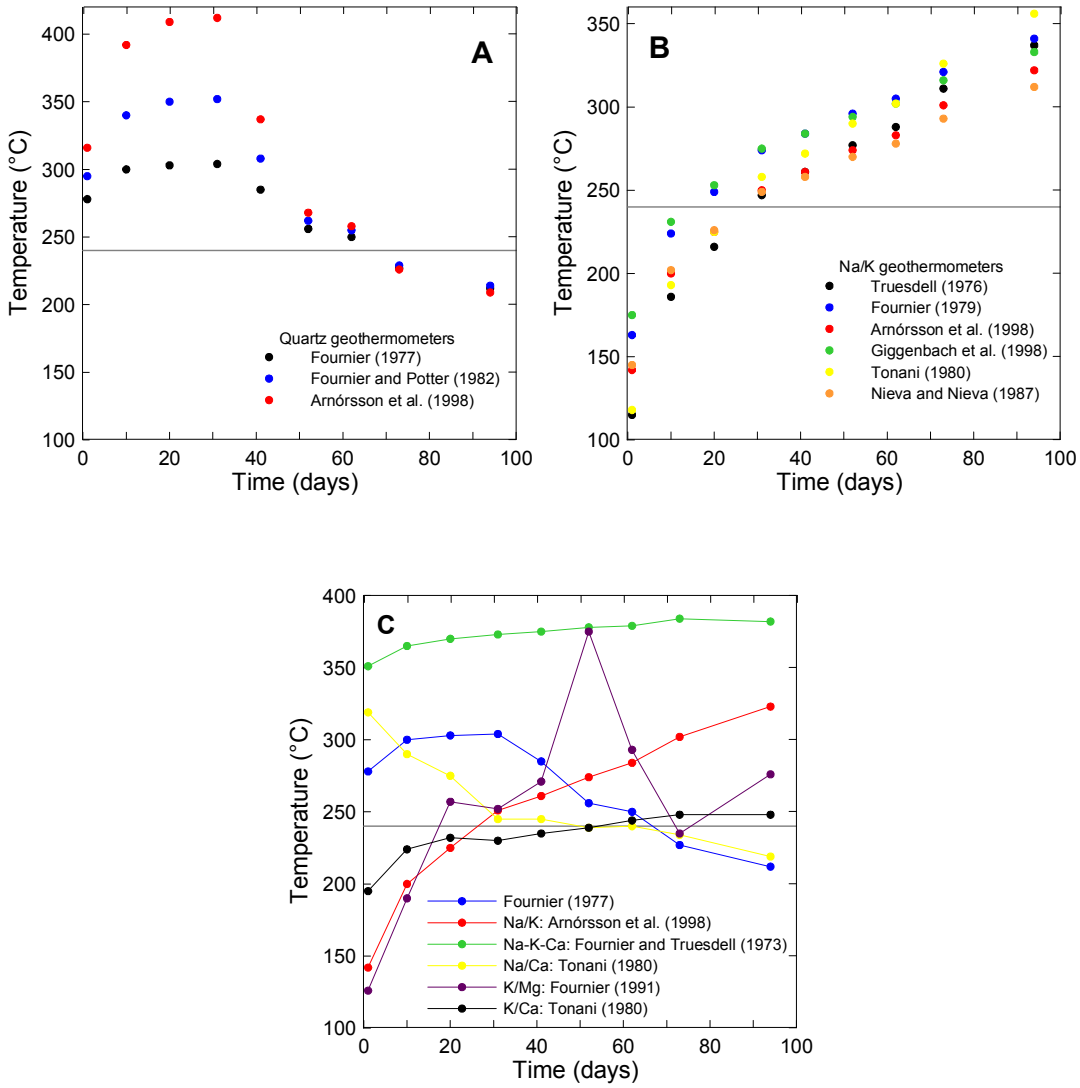

Figure 11. The calculated geothermometry temperatures based on the Askja 1875 94-day experiment. A) Quartz. B) Na/K. C) Other cation geothermometers.

The approach carried out in this study to gain insight into this overall process by combining laboratory experiments with reaction modelling in a closed system has mostly been conducted for mafic rock systems at <100°C (see Gysi and Stefánsson, 2011 and references therein), but less has been done under geothermal conditions for intermediate and silicic rock composition. Specific reactions including smectites to mixed illite-smecite transitions to mica has been studied experimentally for example (e.g. Inoue et al., 1992; Altaner and Ylagan, 1997), but less has been done on the overall reactions as a function of extent of reaction. It is, therefore, very interesting to see the effects of rock composition as well as temperature on the process of water-rock interaction and extent of reaction, particularly because of the similarities in mineral assemblages observed between geothermal systems hosted in mafic, intermediate and silicic rocks with, however,

important differences in for example clay mineralogy (e.g. Browne, 1978; Shikazono and Kawahata, 1987; Lonker et al., 1990; Flexser, 1991; Beaufort et al., 1992; Yang et al., 2001; Inoue et al., 2004; Mas et al., 2006).

The schematic picture of the effect of extent of reaction on silicic rock alteration is shown in Figure 12. It is based primarily on the models for Askja sample. The alteration at 240°C may be divided into three stages based on secondary mineralogy and elemental composition. Stage I (immature) is characterised by formation of insoluble phases including clays and sulphides. Upon progressive rock leaching Stage II is reached, that is characterised by the appearance of quartz and zeolites. Eventually, Stage III is reached at considerable reaction progress (~1 mol of silicic glass per kg of water) whereas smectites and zeolites are replaced by other aluminium silicates including epidote, feldspars, chlorite and carbonates. Stage III closely matches the commonly observed secondary mineralogy associated with geothermal systems at ~240°C (e.g. Browne, 1978). However, to reach this stage, up to 1 mole of glass needs to dissolve in one kg of water; this corresponds to about 100 g of rock. The composition of the clays seems to be somewhat dependent on both system composition (we have only studied the effects of small rock compositional variations) and extend of reaction. For the Hekla samples, the clays that seemed to predominate were illite and/or mixed illite-smectites and Fe-rich chlorites, whereas for Askja sample montmorillonite and Fe(Mg)-chlorite was formed rather than illite. Based on the experimental results, the presence of some of the minerals is also unclear including low-albite and microcline, pyrite and epidote. According to the models, these should be important secondary minerals upon extensive rock alteration, and hence much longer experiments are needed to reveal their formation. In addition, formation of pyrite is dependent on the initial H_2S concentration and possible H_2S oxidation.

The elemental mobilities calculated based on modelled solution concentrations over the sum of initial and stoichiometrically released elemental concentrations are further shown in Figure 12. The mobility of most elements is sharply decreased during Stage I to II, whereas the Na and K are not quantitatively taken up by secondary minerals until Stage III.

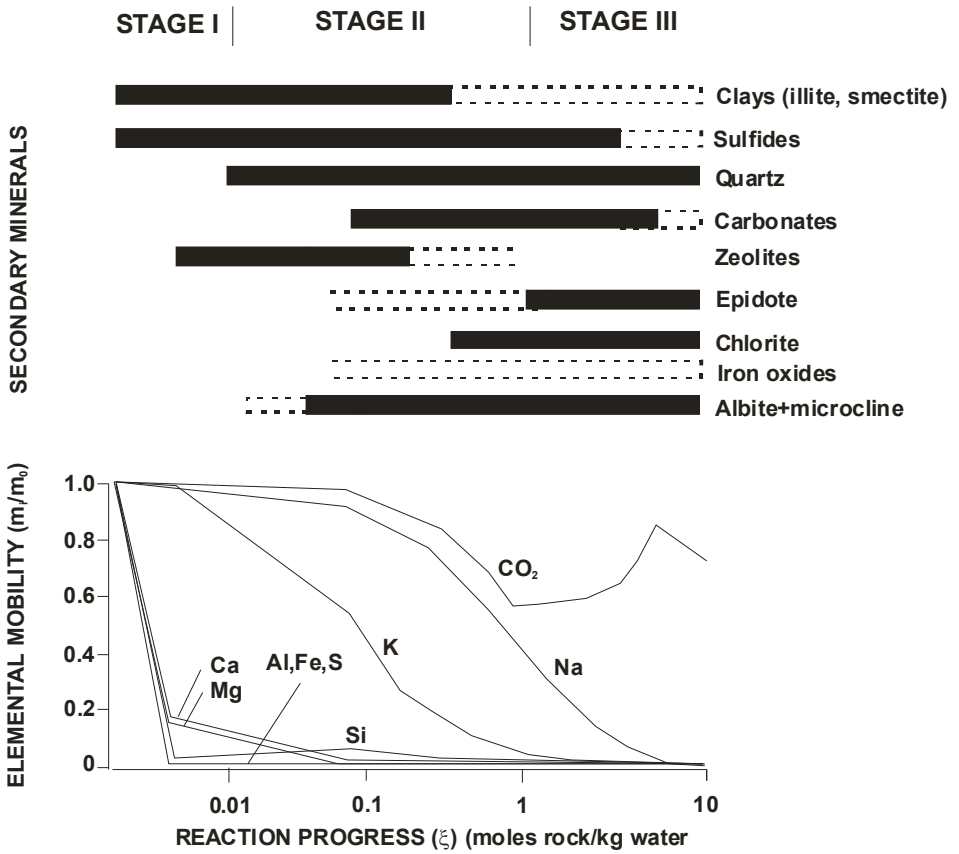

Figure 12. The effect of extent of reaction on the secondary mineralogy and elemental mobility during water-rock interaction of silicic rocks at 240°C.

The overall conclusion is that considerable rock leaching is needed to obtain the secondary mineralogy commonly associated with geothermal alteration of silicic rocks. For systems that are more immature, the secondary mineralogy is different compared to later stages, as well as elemental mobilities and concentrations. This in turns affects the overall solute concentrations that are reflected in difficulties applying geothermal geothermometry, for example, in immature systems. The variations of clay composition and mineralogy commonly observed in natural geothermal systems hosted by silicic rocks dominated by illite and mixed illite-smectites and chlorites seems to be largely dependent on rock composition and to lesser extent on the extent of reaction. The composition of the fluids (salinity) and temperature may also play an important role; however, this will be the subject of future work.

5 Summary and conclusions

Water-rock interaction and geothermal alteration depends on various factors including temperature, pressure, rock and fluid composition, permeability, time (extent of reaction), hydrology and number of superimposed hydrothermal regimes, among others. The aim of this contribution was to study the effects of extent of reaction on silicic rock alteration and the associated water chemistry under geothermal conditions.

Batch type experiments were conducted at 240°C and initial ~9 water/rock ratios on water-rock interaction of two natural volcanic glasses, dacite from Askja and rhyolite from Hekla. The initial solutions consisted of non-thermal ground-waters spiked with CO_2, H_2S and NaCl to approach geothermal conditions, and the water chemistry and mineralogy studied upon reactions of several weeks to months. In addition, reaction path simulations were conducted in order to get further insight into the effects of progressive silicic rock interaction at isothermal conditions.

After 30 days of experiment, the Askja glass (A75) appeared relatively fresh and apart from showing indications of dissolved surfaces, there was very little mass of alteration product consisting mainly of smectites and zeolites. For the longer Askja experiment lasting 94 days, a considerable amount of alteration products was observed. Secondary minerals included quartz, anhydrite, clays like montmorillonite and chlorite, zeolites like analcime and phillipsite and possible traces of fluorite and anatase. For the Hekla glass (H3W) considerable alteration was observed after 42 days and consisted of quartz, clays consisting of illite and possibly also mixed illite-smectites and chlorite, and zeolites like analcime. In addition, traces of anatase, fluorite and possible calcite may also have been present. The observed mineralogy is in reasonable agreement with alteration associated with natural geothermal systems hosted by silicic rocks at ~250°C (e.g. Lonker et al., 1990; Reyes, 1990; Harvey and Browne, 1991; Beaufort et al., 1992; Inoue et al., 2004; Mas et al., 2006). The results for the Askja and Hekla samples also suggest that fine compositional variations of the major ions including K, Fe, Ca and Mg have large influences on the predominant clay composition. For the Askja model, montmorillonite and Mg-chlorite predominated whereas for the Hekla model, illite was the most important clay with some Fe-chlorite as well. Based on elemental mobility, it was concluded that the dissolution of silicic rocks under geothermal conditions is incongruent. Aluminium, Fe and Mg showed a reduced mobility compared to B during all the experiments suggesting that these elements were quantitatively incorporated into secondary minerals including zeolites like analcime, clays like montmorillonite, illite and chlorite. Sodium, Ca and Si all showed reduced mobility upon reaction progress. Silica is considered to have entered into various Al-Si minerals and quartz whereas Na and Ca were incorporated into minerals like analcime, montmorillonite, calcite and anhydrite. The results are in reasonable agreement with the mineralogical observations and mineral saturation state, with many of the observed minerals found to be saturated and/or supersaturated.

The results of the experiments were further constrained by comparing them with the results of reaction path modelling. In the simulations, silicic glass (1-10 moles) was dissolved in series of steps. The results indicated that the appearance of various minerals in a closed system is initially a function of reaction progress. Furthermore, comparison show that precipitation kinetics may be of importance for some elements like Si, K and Na

whereas the exact Mg, Fe and Ca composition of the primary material plays a significant role in the mass and composition of secondary Ca, Mg and Fe containing aluminium silicates and oxides. The results between the Askja and Hekla sample also show that fine compositional variations of the major ions including K, Fe, Ca and Mg have large influences on the predominant clay composition.

Based on the experimental results and reaction path modelling, the alteration of silicic rocks at 240°C was divided into three stages. Stage I (immature) is characterised by formation of insoluble phases including clays and sulphides. Upon progressive rock leaching Stage II is reached with the appearance of quartz and zeolites. Stage III is reached at considerable reaction progress (>1 mol of silicic glass per kg water) whereas clays and zeolites are replaced by other aluminium silicates including epidote, feldspars, chlorite and carbonates. The mobility of most elements is sharply decreased during Stage I to II, whereas the Na and K are not quantitatively taken up by secondary minerals until in Stage III. This last stage closely matches the commonly observed secondary mineralogy associated with geothermal systems at ~240°C (e.g. Browne, 1978). Moreover, the composition of the clays seems to be somewhat dependent on both system composition (we have only studied the effects of small rock compositional variations) and extend of reaction with rocks higher in Fe and Mg forming montmorillonite and chlorite whereas rocks lower in Mg and Fe tend to form illite and mixed illite-smectite.

The conclusion of the study is that alteration of silicic rocks under isothermal conditions is a function of rock and fluid composition as well as extent of reaction. The water-rock ratio is particularly important during early stages of alteration whereas extensive water-rock interaction proceeds into a phase whereas the secondary mineralogy does not change much with further alteration, only the mass. Moreover, the comparison of the experimental results with the reaction path simulations suggests that kinetics plays an important role in formation of some secondary minerals under geothermal conditions. This in turns has some important implications for example in the application of alteration mineralogy and fluid chemistry for estimation of past and present reservoir temperatures.

References

Altaner, S.P. and Ylagan, R.F., 1997. Comparison of structural models of mixed-layer illite/smectite and reaction mechanisms of smectite illitization. Clays and Clay Minerals, 45(4): 517-533.

Arnórsson, S. and Andrésdóttir, A., 1995. Processes controlling the distribution of boron and chlorine in natural waters in Iceland. Geochimica Et Cosmochimica Acta, 59(20): 4125-4146.

Arnórsson, S., Andrésdóttir, A., Gunnarsson, I. and Stefánsson, A., 1998. New calibration for the quartz and Na/K geothermometers-valid in the range 0-350°C, Geoscience Society of Iceland Annual Meeting, April 1994., pp. 42-43 (in Icelandic).

Arnórsson, S., Bjarnason, J.Ö., Giroud, N., Gunnarsson, I. and Stefánsson, A., 2006. Sampling and analysis of geothermal fluids. Geofluids, 6(3): 203-216.

Arnórsson, S., Gunnlaugsson, E. and Svavarsson, H., 1983. The chemistry of geothermal waters in Iceland. II. Mineral equilibria and independent variables controlling water compositions. Geochimica Et Cosmochimica Acta, 47(3): 547-566.

Arnórsson, S. and Stefánsson, A., 1999. Assessment of feldspar solubility constants in water in the range 0 degrees to 350 degrees C at vapor saturation pressures. American Journal of Science, 299(3): 173-209.

Beaufort, D., Patrier, P., Meunier, A. and Ottaviani, M.M., 1992. Chemical variations in assemblages including epidote and/or chlorite in the fossil hydrothermal system of Saint Martin (Lesser Antilles). Journal of Volcanology and Geothermal Research, 51(1-2): 95-114.

Bethke, C.M., Vergo, N. and Altaner, S.P., 1986. Pathways of smectites illitization. Clays and Clay Minerals, 34(2): 125-135.

Bird, D.K., Schiffman, P., Elders, W.A., Williams, A.E. and McDowell, S.D., 1984. Calc-silicate mineralization in active geothermal systems. Economic Geology, 79(4): 671-695.

Browne, P.R.L., 1978. Hydrothermal Alteration in Active Geothermal Fields. Annual Review of Earth and Planetary Sciences, 6: 229-250.

Cathelineau, M. and Nieva, D., 1985. A Chlorite Solid-Solution Geothermometer - the Los-Azufres (Mexico) Geothermal System. Contributions to Mineralogy and Petrology, 91(3): 235-244.

Davis, A.C., Bickle, M.J. and Teagle, D.A.H., 2003. Imbalance in the oceanic strontium budget. Earth and Planetary Science Letters, 211(1-2): 173-187.

Dolejs, D. and Wagner, T., 2008. Thermodynamic modeling of non-ideal mineral-fluid equilibria in the system Si-Al-Fe-Mg-Ca-Na-K-H-O-Cl at elevated temperatures and pressures: Implications for hydrothermal mass transfer in granitic rocks. Geochimica Et Cosmochimica Acta, 72(2): 526-553.

Elders, W.A., Hoagland, J.R. and Williams, A.E., 1981. Distribution of hydrothermal mineral zones in the Cerro Prieto geothermal field of Baja California, Mexico. Geothermics, 10(3-4): 245-253.

Ellis, A.J., 1970. Quantitative interpretation of chemical characteristics of hydrothermal systems. Geothermics, 2(Part 1): 516-528.

Essene, E.J. and Peacor, D.R., 1995. Clay mineral thermometry. A critical perspective. Clays and Clay Minerals, 43(5).

Flexser, S., 1991. Hydrothermal alteration and past and present thermal regimes in the western moat of Long Valley caldera. Journal of Volcanology and Geothermal Research, 48(3-4): 303-318.

Fournier, R.O., 1977. Chemical Geothermometers and mixing models for geothermal systems. Geothermics, 5: 41-50.

Fournier, R.O., 1991. Water geothermometers applied to geothermal energy. In: F. D´Amore (Editor), Applications of geochemistry in geothermal reservoir development. UNITAR publication, Rome, pp. 37-69.

Fournier, R.O. and Potter, R.W.I., 1979. Magnesium correction to the Na---K---Ca chemical geothermometer. Geochimica Et Cosmochimica Acta, 43(9): 1543-1550.

Fournier, R.O. and Potter, R.W.I., 1982. A revised and expanded silica (quartz) geothermometer. Geothermal Research Council Bulletin, 11: 3-9.

Fournier, R.O. and Truesdell, A.H., 1973. An empirical Na---K---Ca geothermometer for natural waters. Geochimica Et Cosmochimica Acta, 37(5): 1255-1275.

Franzson, H., Thordason, S., Bjornsson, G., Gudlaugsson, S.T., Richter, B., Fridleifsson, G.O. and Thorhallsson, S., 2002. Reykjanes high-temperature field, SW-Iceland. Geology and hydrothermal alteration of well RN-10, Proceedings 27th Workshop on Geothermal Reservoir Engineering, Stanford University.

Giggenbach, W.F., 1980. Geothermal Gas Equilibria. Geochimica Et Cosmochimica Acta, 44(12): 2021-2032.

Giggenbach, W.F., 1981. Geothermal Mineral Equilibria. Geochimica Et Cosmochimica Acta, 45(3): 393-410.

Giggenbach, W.F., 1984. Mass transfer in hydrothermal alteration systems--A conceptual approach. Geochimica Et Cosmochimica Acta, 48(12): 2693-2711.

Giggenbach, W.F., Minissale, A.A. and Scandiffio, G., 1988. Isotopic and chemical assessment of geothermal potential of the Colli Albani are, Latium region, Italy. Applied Geochemistry, 3: 475-486.

Gunnarsson, B., Marsh, B.D. and Jr., H.P.T., 1998. Generation of Icelandic rhyolites: silics lavas from the Torfajökull central volcano. Journal of Volcanology and Geothermal Research, 83: 1-45.

Gysi, A.P. and Stefánsson, A., 2011. CO2–water–basalt interaction: II. Low-temperatures reaction path modelling and comparison with experimental and natural data. Geochim. Cosmochim. Acta (submitted).

Harvey, C.C. and Browne, P.R.L., 1991. Mixed-layer clay geothermometry in the Wairakei geothermal field, New Zealand. Clays and Clay Minerals, 39: 614-621.

Hedenquist, J.W., Arribas, A. and Reynolds, T.J., 1998. Evolution of intrusion-centered hydrothermal systems and epithermal Cu-Au deposits, Philippines. Economic Geology, 93: 374-404.

Heinrich, C.A., Walshe, J.L. and Harrold, B.P., 1996. Chemical mass transfer modelling of ore-forming hydrothermal systems: Current practise and problems. Ore Geology Reviews, 10(3-6): 319-338.

Helgeson, H.C., 1968. Evaluation of irreversible reactions in geochemical processes involving minerals and aqueous solutions--I. Thermodynamic relations. Geochimica Et Cosmochimica Acta, 32(8): 853-877.

Helgeson, H.C., 1979. Mass transfer among minerals and hydrothermal solutions. In: H.L. Barnes (Editor), Geochemistry of Hydrothermal Ore Deposits. Wiley, New York, pp. 568 – 610.

Henley, R.W. and Ellis, A.J., 1983. Geothermal Systems Ancient and Modern - a Geochemical Review. Earth-Science Reviews, 19(1): 1-50.

Henneberger, R.C. and Browne, P.R.L., 1988. Hydrothermal alteration and evolution of the Ohakuri hydrothermal system, Taupo volcanic zone, New Zealand. Journal of Volcanology and Geothermal Research, 34(3-4): 211-231.

Hreggvidsdóttir, H., 1987. The green schist to amphibolite facies transition in the Nesjavellir geothermal system, Southwest Iceland. MSc. thesis, University of Stanford, 66 pp.

Inoue, A., Meunier, A. and Beaufort, D., 2004. Illite - smectite mixed layer minerals in felsic volcaniclastic rocks from drill cores, Kakkonda, Japan. Clays and Clay Minerals, 52(1): 66-84.

Inoue, A. and Utada, M., 1983. Further investigations of a conversion series of dioctahedral mica/smectite in the Shinzan hydrothermal alteration area, northeast Japan. Clays and Clay Minerals, 31: 401-412.

Inoue, A., Utada, M. and Wakita, K., 1992. Smectite-to-illite conversion in natural hydrothermal systems. Applied Clay Science, 7(1-3): 131-145.

Ji, J. and Browne, P.R.L., 2000. Relationship between illite crystallinity and temperature in active geothermal systems of New Zealand. Clays and Clay Minerals, 48(1): 139-144.

Jónasson, K., 2007. Silicic vulcanism in Iceland: Composition and distribution within the active volcanic zones. Journal of Geodynamics, 43: 101-117.

Kristmannsdóttir, H., 1979. Alteration of basaltic rocks by geothermal activity at 100-300°C. In: M. Mortland and V. Farmer (Editors), Developments in Sedimentology. Elsevier, Amsterdam, pp. 359-367.

Kristmannsdóttir, H. and Tómasson, J., 1978. Zeolite zones in geothermal areas in Iceland. In: S. L.B. and M.F. A. (Editors), Natural zeolites; occurrence, properties and use. Pergamon Press, New York, pp. 277-284.

Larsen, G., Dugmore, A. and Newton, A., 1999. Geochemistry of historical-age silicic tephras in Iceland. The Holocene, 9: 463-471.

Larsson, D., Grönvold, K., Oskarsson, N. and Gunnlaugsson, E., 2002. Hydrothermal alteration of plagioclase and growth of secondary feldspar in the Hengill Volcanic Centre, SW Iceland. Journal of Volcanology and Geothermal Research, 114(3-4): 275-290.

Le Bas, M.J., Le Maitre, R.W., Streckeisen, A. and Zanettin, B., 1986. A chemical classification of volcanic rocks based on the total alkali-silica diagram. Journal of Petrology, 27: 745-750.

Lesher, C.M., Gibson, H.L. and Campbell, I.H., 1986. Composition-Volume Changes during Hydrothermal Alteration of Andesite at Buttercup-Hill, Noranda-District, Quebec. Geochimica Et Cosmochimica Acta, 50(12): 2693-2705.

Lonker, S.W., Fitz Gerald, J.D., Hedenquist, J.W. and Walshe, J.L., 1990. Mineral-Fluid Interactions in the Broadlands-Ohaaki Geothermal System, New-Zealand. American Journal of Science, 290(9): 995-1068.

Lonker, S.W., Franzson, H. and Kristmannsdottir, H., 1993. Mineral-Fluid Interactions in the Reykjanes and Svartsengi Geothermal Systems, Iceland. American Journal of Science, 293(7): 605-670.

MacDonald, R., Sparks, R.S.J., Sigurdsson, H., Matey, D.P., McGarvie, D.W. and Smith, R.L., 1987. The 1975 eruption of Askja volcano, Iceland: combined fractional crystallization and selective contamination in the generation of rhyolitic magma. Mineralogical Magazine, 51(360): 183-202.

Marini, L., 2006. Geological Sequestration of Carbon Dioxide: thermodynamics, kinetics and reaction path modelling. Developments in Geochemistry, Volume 11. Elsevier, 453 pp.

Marks, N., Schiffman, P., Zierenberg, R.A., Frannon, H. and Fridleifsson, G.O., 2010. Hydrothermal alteration in the Reykjanes geothermal system: Insights from Iceland deep drilling program well RN-17. Journal of Volcanology and Geothermal Research, 189(1-2): 172-190.

Mas, A., Guisseau, D., Patrier Mas, P., Beaufort, D., Genter, A., Sanjuan, B. and Girard, J.P., 2006. Clay minerals related to the hydrothermal activity of the Bouillante geothermal field (Guadeloupe). Journal of Volcanology and Geothermal Research, 158(3-4): 380-400.

McDowell, S.D. and Elders, W.A., 1980. Authigenic Layer Silicate Minerals in Borehole Elmore-1, Salton-Sea Geothermal-Field, California, USA. Contributions to Mineralogy and Petrology, 74(3): 293-310.

Mehegan, J.M., Robinson, P.T. and Delaney, J.R., 1982. Secondary Mineralization and Hydrothermal Alteration in the Reydarfjordur Drill Core, Eastern Iceland. Journal of Geophysical Research, 87(Nb8): 6511-6524.

Neuhoff, P.S., Fridriksson, T., Arnorsson, S. and Bird, D.K., 1999. Porosity evolution and mineral paragenesis during low-grade metamorphism of basaltic lavas at Teigarhorn, eastern Iceland. American Journal of Science, 299(6): 467-501.

Nieva, D. and Nieva, R., 1987. Developments in geothermal energy in Mexico, Part 12. A cationic geothermometer for prospecting of geothermal resources. Heat and Recovery Systems & CHP 7: 243-258.

Nordstrom, D.K. and Munoz, J.L., 2006. Geochemical Thermodynamics. -2nd ed. The Blackburn Press.

Palmer, M.R. and Edmond, J.M., 1989. The Strontium Isotope Budget of the Modern Ocean. Earth and Planetary Science Letters, 92(1): 11-26.

Parkhurst, D.L. and Appelo, C.A.J., 1999. User's guide to PHREEQC (Version 2)--a computer program for speciation, batch-reaction, one-dimensional transport, and inverse geochemical calculations. Report 99-4259, U.S. Geological Survey, Water-Resources Investigations.

Poppe, L.J., Paskevich, V.F., Hathaway, J.C. and Blackwood, D.S., 2002. A Laboratory Manual for X-Ray Powder Diffraction. Open-File Report 01-041, U. S. Geological Survey.

Reyes, A.G., 1990. Petrology of Philippine geothermal systems and the application of alteration mineralogy to their assessment. Journal of Volcanology and Geothermal Research, 43: 279-309.

Roberson, H.E. and Lahann, R.W., 1981. Smectite to Illite Conversion Rates - Effects of Solution Chemistry. Clays and Clay Minerals, 29(2): 129-135.

Rózsa, P., Szöór, G., Elekes, Z., Gratuze, B., Uzonyi, I. and Kiss, Á.Z., 2006. Comparative geochemical studies of obsidian samples from various localities. Acta Geologica Hungarica, 49(1): 73-87.

Schiffman, P. and Fridleifsson, G.O., 1991. The smectite–chlorite transition in drillhole NJ-15, Nesjavellir geothermal field, Iceland: XRD, BSE and electron microprobe investigations. Journal of Metamorphic Geology, 9(6): 679-696.

Shikazono, N. and Kawahata, H., 1987. Compositional Differences in Chlorite from Hydrothermally Altered Rocks and Hydrothermal Ore-Deposits. Canadian Mineralogist, 25: 465-474.

Sigvaldason, G., 1973. The petrology of Hekla and origin of silicic rocks in Iceland, Meeting of the Icelandic Geoscience Society, Reykjavík, Iceland, pp. 70.

Sigvaldason, G., 2002. Volcanic and tectonic processes coinciding with glaciation and crustal rebound: an early Holocene rhyolitic eruption in Dyngjufiöll volcanic centre and the formation of the Askja caldera, north Iceland. Bulletin of Volcanology, 64: 192-205.

Sigvaldason, G. and Óskarsson, N., 1976. Chlorine in basalts from Iceland. Geochimica Et Cosmochimica Acta, 40: 777-789.

Sigvaldason, G., Sigurdsson, H. and Sparks, R.S.J., 1981. Petrology of the rhyolitic and mixed magma ejecta from 1875 eruption of Askja, Iceland. Journal of Petrology, 22: 41-84.

Smith, A.K. and Simon, J.I., 2004. Boron isotopic variations in hydrous rhyolitic melts: a case study from Long Valley, California. Contributions to Mineralogy and Petrology, 146: 590-605.

Sparks, R.S.J., Wilson, L.W. and Sigurdsson, H., 1981. The pyroclastic deposits of the 1875 Eruption of Askja, Iceland. Philosophical Transactions of the Royal Society of London. Series A, Mathematical and Physical Sciences, 299(1447): 241-273.

Stefánsson, A., 2010. Low-temperature alteration of basalts – the effects of temperatre, acids and extent of reaction on mineralization and water chemistry. Jökull, 60: 165-184.

Stefánsson, A. and Arnórsson, S., 2000. Feldspar saturation state in natural waters. Geochimica Et Cosmochimica Acta, 64(15): 2567-2584.

Stefánsson, A. and Arnórsson, S., 2002. Gas pressures and redox reactions in geothermal fluids in Iceland. Chemical Geology, 190(1-4): 251-271.

Stefánsson, A., Arnórsson, S., Gunnarsson, I. and Kaasalainen, H., 2009. Sequestration of H2S from the Hellisheidi power plant — a geochemical study. Sci. Inst. Report RH-14-2009. 84 pp.

Stefánsson, A., Arnórsson, S., Gunnarsson, I., Kaasalainen, H. and Gunnlaugsson, E., 2011. The geochemistry and sequestration of H2S into the geothermal system at Hellisheidi, Iceland. Journal of Volcanology and Geothermal Research, 202(3-4): 179-188.

Stefánsson, A., Arnórsson, S. and Sveinbjörnsdóttir, Á.E., 2005. Redox reactions and potentials in natural waters at disequilibrium. Chemical Geology, 221(3-4): 289-311.

Sveinbjörnsdóttir, A.E., Coleman, M.L. and Yardley, B.W.D., 1986. Origin and history of hydrothermal fluids of the Reykjanes and Krafla geothermal fields, Iceland. A stable isotope study. Contributions to Mineralogy and Petrology, 94: 99-109.

Tonani, F., 1980. Some remarks on the application of geochemical techniques in geothermal exploration, Proceedings of the 2nd International Seminar on the Results of E.C. Geothermal Energy Research. Reidel Publishing Co, Strasbourg, pp. 428-443.

Truesdell, A.H., 1976. Summary of Section III. Geochemical Techniques in Exploration, Second United Nations Symposium on the Development and Use of Geothermal Resources, San Francisco, pp. 53-79.

Weisenberger, T. and Selbekk, R.S., 2009. Multi-stage zeolite facies mineralization in the Hvalfjordur area, Iceland. International Journal of Earth Sciences, 98(5): 985-999.

Wolff-Boenisch, D., 2004. Data on 17 Icelandic volcanic glasses and 1 Californian ignimbrite. RH-03-2004, Science Institute, University of Iceland.

Wolff-Boenisch, D., Gislason, S.R., Oelkers, E.H. and Putnis, C.V., 2004. The dissolution rates of natural glasses as a function of their composition at pH 4 and 10.6, and temperatures from 25 to 74°C. Geochimica Et Cosmochimica Acta, 68(23): 4843-4858.

Yang, K., Browne, P.R.L., Huntington, J.F. and Walshe, J.L., 2001. Characterising the hydrothermal alteration of the Broadlands-Ohaaki geothermal system, New Zealand, using short-wave infrared spectroscopy. Journal of Volcanology and Geothermal Research, 106(1-2): 53-65.

Appendix A. Results of XRD analysis

The following samples were characterized using a Philips® 1050/1140 x-ray diffractometer with a Cu anode and PW 1964 scintillation counter; ran at 20 mA and 40 kV with a scanning speed of 1°/2θ/min.

Askja 1875 (A75) 94-day experiment

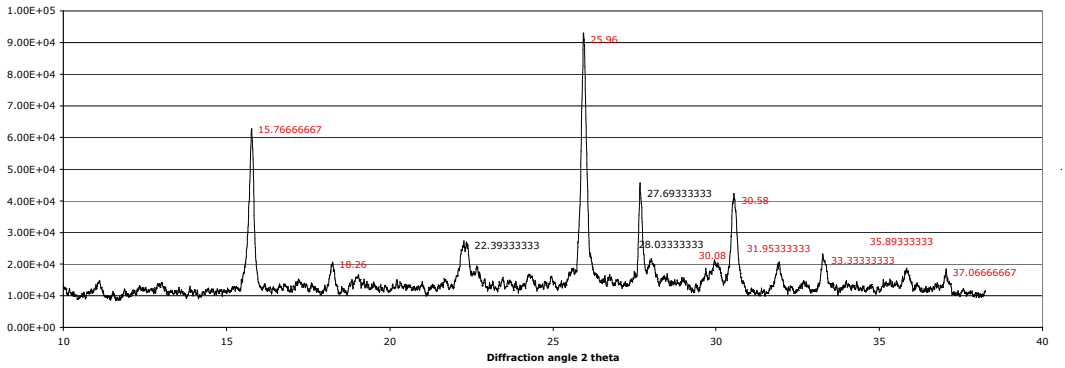

Sample A75(3)-BM-1: bulk bottom material. Analcime and albite.

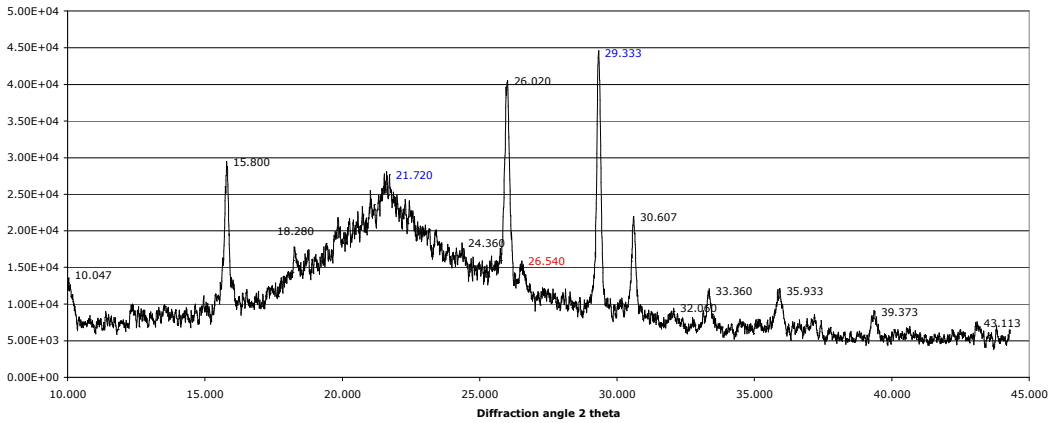

Sample A75(3)-BM-2: bulk bottom material. Large amounts of amorphous silica (baseline) and analcime. Calcite and traces of quartz.

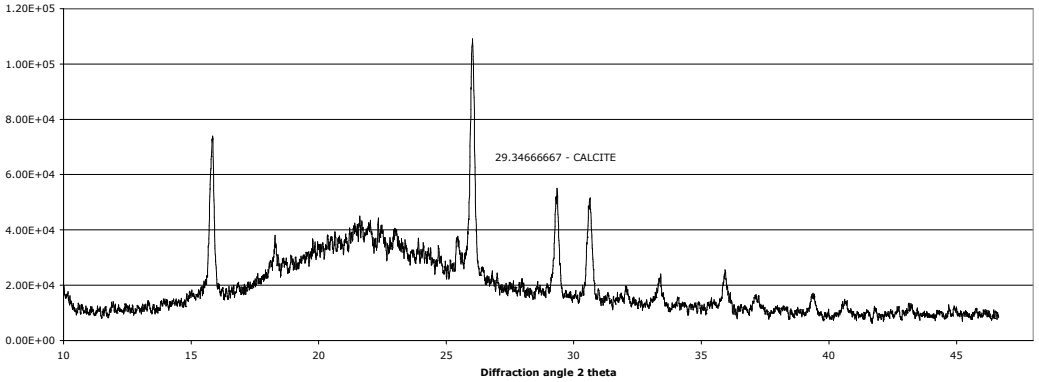

Sample A75(3)-WS: wall scales. Amorphous silica, analcime and minor calcite.

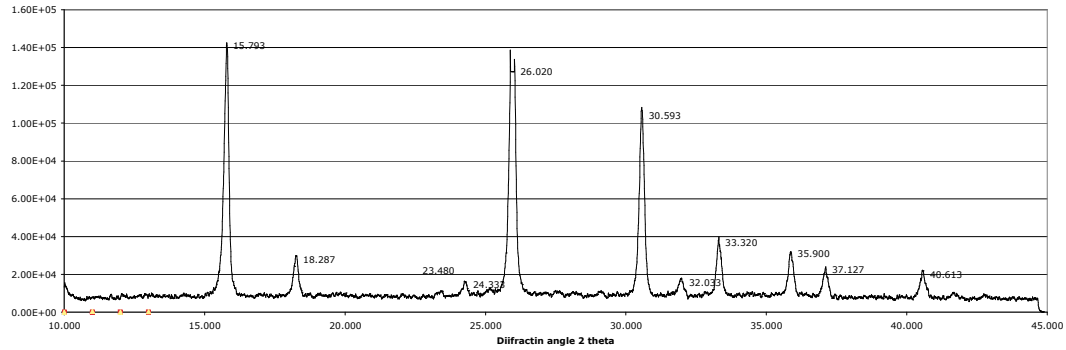

Sample A75(3)-PS: pipes scales. Almost pure analcime.

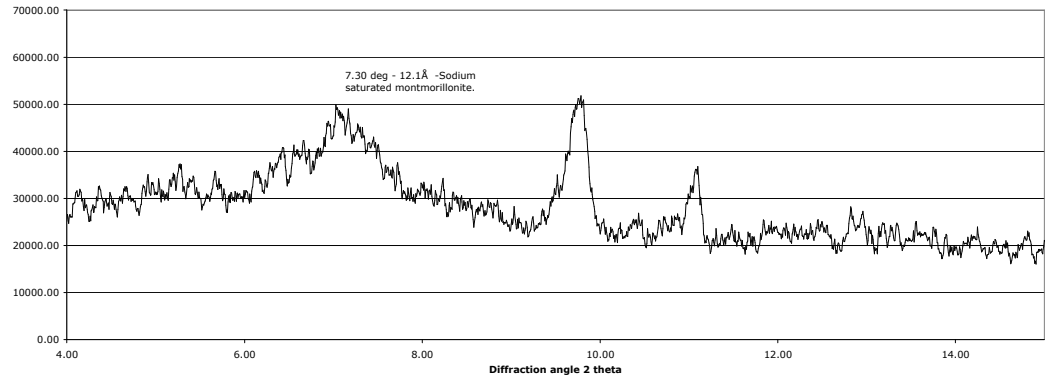

Sample A75(3)-BM-C1: bulk bottom sample, clay separated and untreated. Sodium montmorillonite.

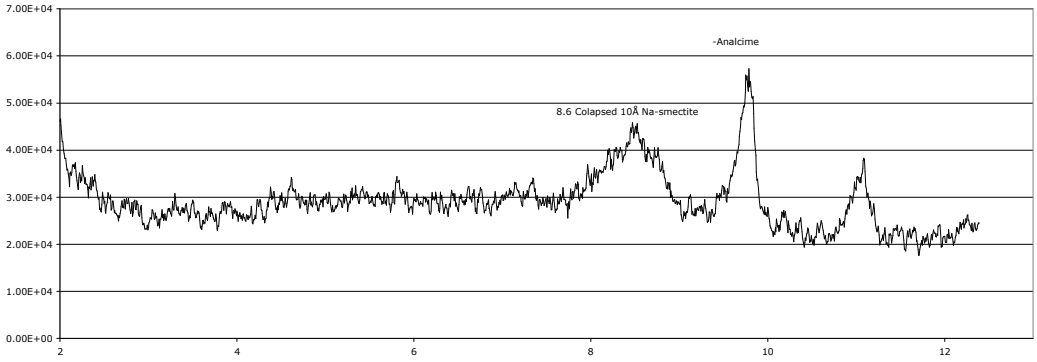

Sample A75(3)-BM-C1: clay separated from bulk bottom sample and untreated up to 200°C. Collapse to 10Å upon heating is typical for a Na-saturated smectite.

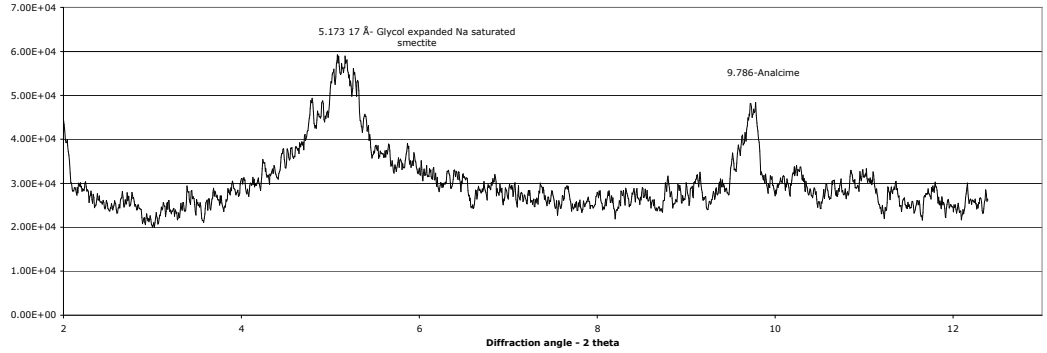

Sample A75(3)-BM-C2: clay separated from bulk bottom sample and treated with ethylene glycol. Expansion to 17Å is typical for a Na-smectite.

The following samples were characterized using a Bruker D8 Focus® with at a Cu anode ran at 40 mA and 40 kV with 2.4°/2θ/min scanning speed. The XRD data are presented as patterns with 2θ value on the x-axis and intensity counts on the y-axis.

Askja 1875 (A75) 30-day experiment

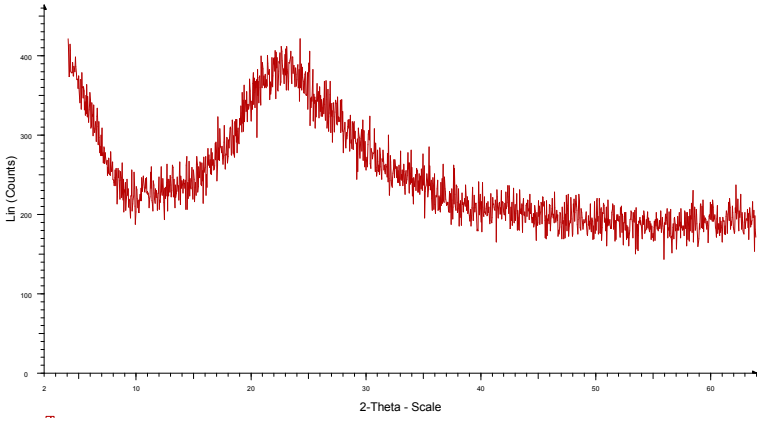

Sample A75: fresh glass, before the experiment. Amorphous material.

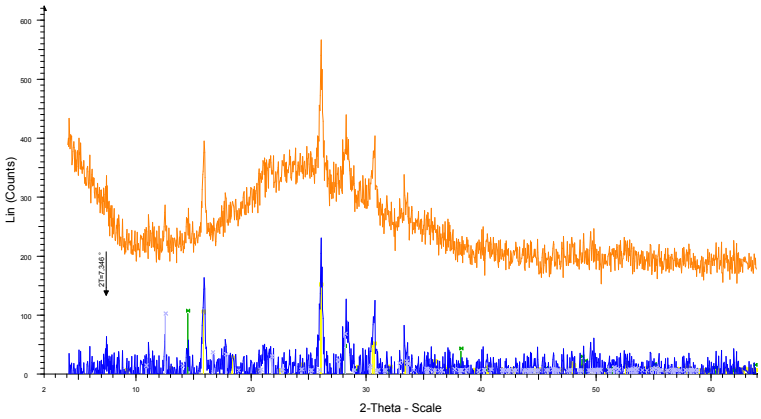

Sample A75(1)-BS: bottom scales. Analcime, boehmite and phillipsite.

Hekla H3W 42-day experiment

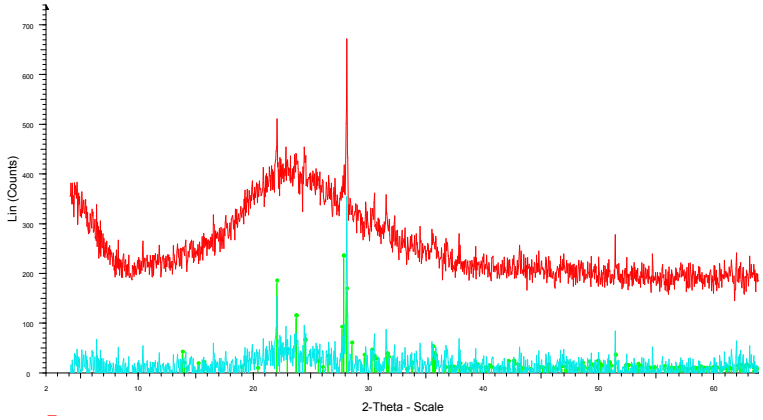

Sample H3W: fresh glass, before the experiment. Amorphous material with albite.

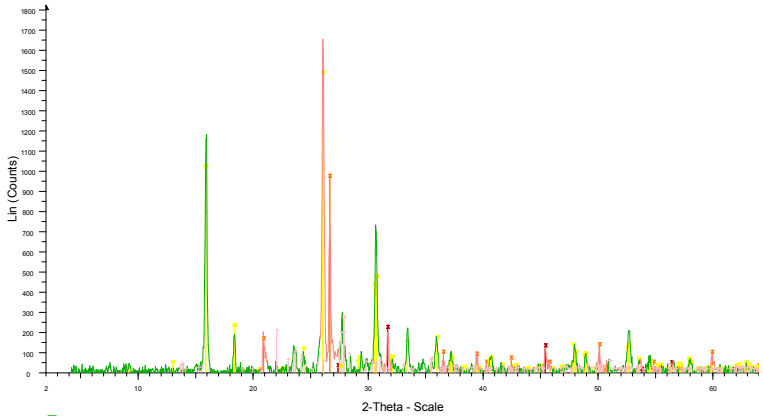

Sample H3W(2)-BS: bottom scales. Halite, quartz, analcime and high albite.

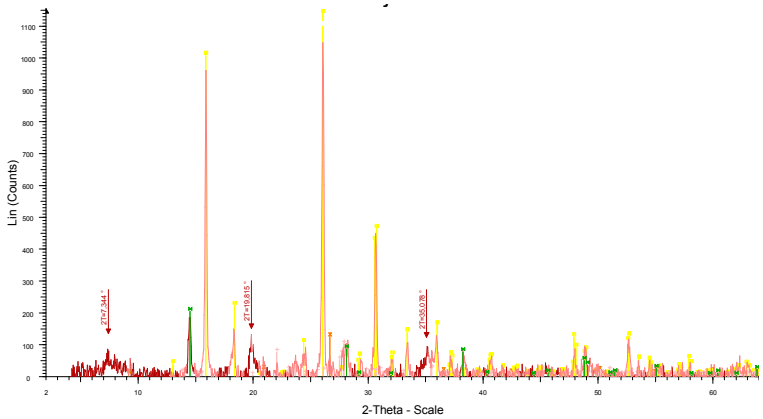

Sample H3W(2)-PS: pipe scales. Quartz, analcime, high albite and boehmite.

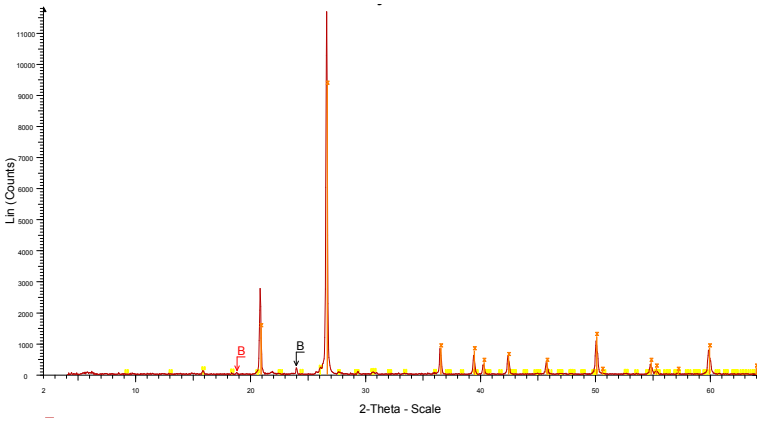

Sample H3W(2)-WS: wall scales. Quartz and analcime.

Appendix B. Results of SEM and EDS analysis

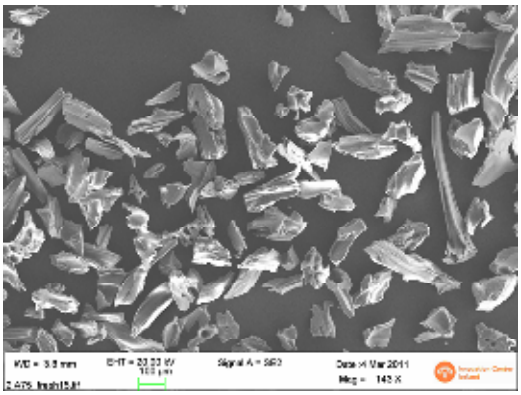

Figure B1: "Fresh" A75 glass.

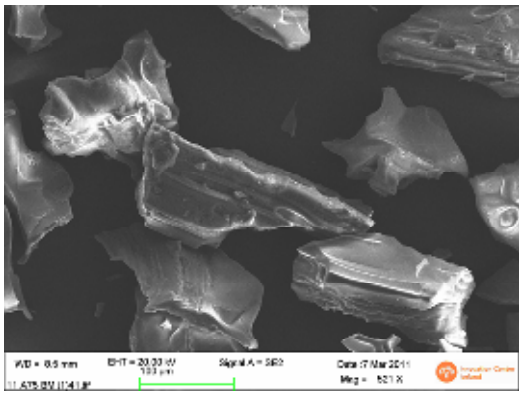

Figure B2: "Pitting" on A75 glass surfaces.

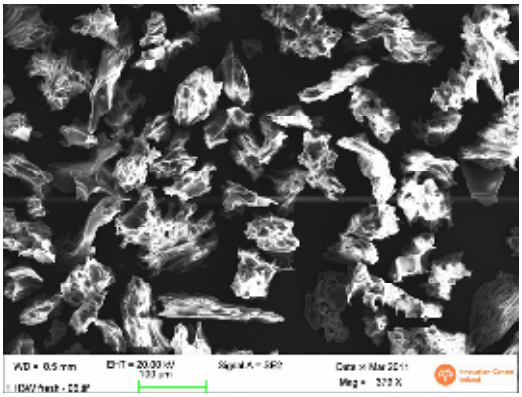

Figure B3: "Fresh" H3W glass.

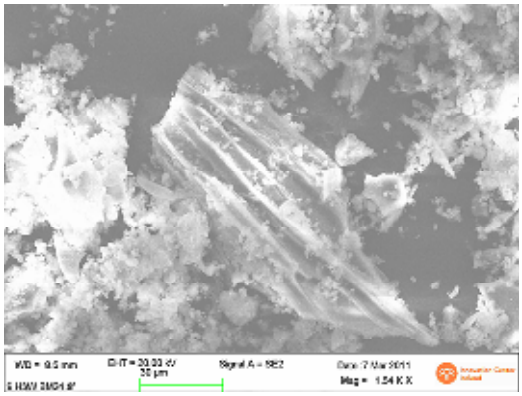

Figure B4: H3W glass fragment covered with alteration products.

Figure B5: Askja 1875 94-day experiment, wall scales.

Anhydrite
Processing option: All elements analyzed (Normalised)
Number of iterations = 4
Standard:
O 2440 CaCO3 3-Nov-2010 02:54 PM
Si 3587 AISI 316 14-Dec-2010 02:09 PM
S 2440 CaSO4 10-Dec-2009 11:36 AM
Ca 2440 Diopside 2-Dec-2010 05:18 PM

Element	Weight%	Atomic%
O K	50.59	69.88
Si K	0.51	0.40
S K	19.98	13.77
Ca K	28.92	15.95
Totals	100.00	

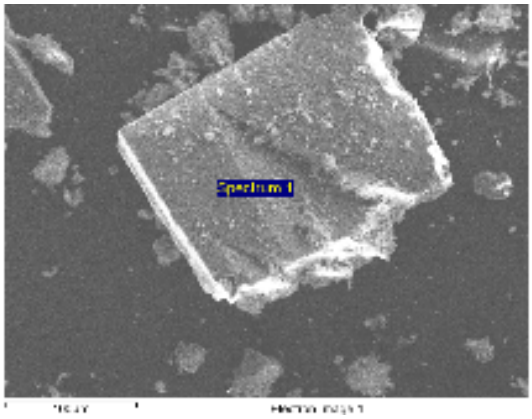

Figure B6: Askja 1875 94-day experiment, bottom scales.

Calcite
Processing option: All elements analyzed (Normalised)
Number of iterations = 6
Standard:
C 2440 CaCO3 3-Nov-2010 02:54 PM
O 2440 CaCO3 3-Nov-2010 02:54 PM
Ca 2440 Diopside 2-Dec-2010 05:18 PM

Element	Weight%	Atomic%
C K	16.66	24.53
O K	58.26	64.40
Ca K	25.08	11.07

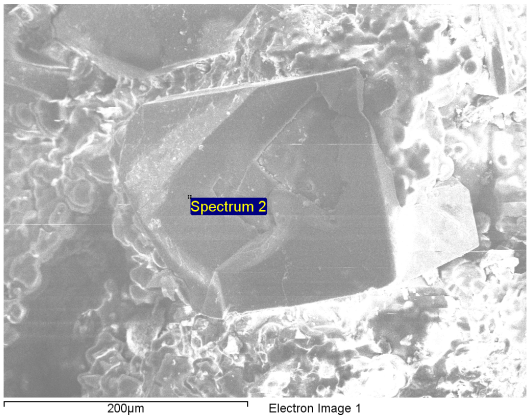

Figure B7: Askja 1875 94-day experiment, wall scales.

Na-rich Si-Al phase with K and Fe.
Probably Na-montorillonite
Processing option: All elements analyzed (Normalised)
Number of iterations = 5
Standard:
O 2440 CaCO3 3-Nov-2010 02:54 PM
Na 2440 Altite 2-Dec-2010 04:15 PM
Al 2440 Altite 2-Dec-2010 04:14 PM
Si 3587 AISI 316 14-Dec-2010 02:09 PM
K 2440 Orthaclase 2-Dec-2010 04:33 PM
Fe 3587 AISI 316 14-Dec-2010 02:09 PM

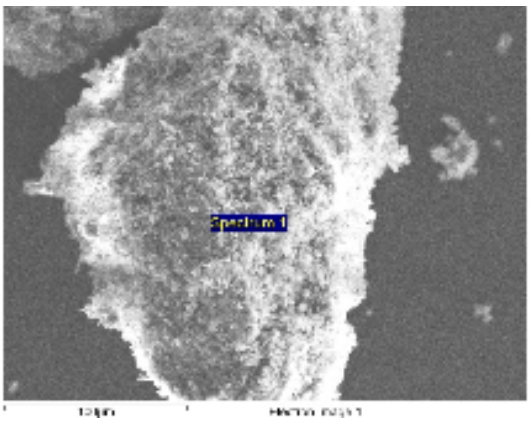

Element	Weight%	Atomic%
O K	61.71	73.42
Na K	4.12	3.41
Al K	4.98	3.51
Si K	28.75	19.48
K K	0.18	0.09
Fe K	0.27	0.09
Totals	100.00	

Figure B8: Askja 1875 30-day experiment, pipe scales.

Fe-rich Si-Al phase containing also Na, K and Mg.
Probably a smectite/chlorite.
Processing option: All elements analyzed (Normalised)
Number of iterations = 4
Standard:
O 2440 CaCO3 3-Nov-2010 02:54 PM
Na 2440 Altite 2-Dec-2010 04:15 PM
Mg 2440 Diopside 2-Dec-2010 04:29 PM
Al 2440 Altite 2-Dec-2010 04:14 PM
Si 3587 AISI 316 14-Dec-2010 02:09 PM
S 2440 CaSO4 10-Dec-2009 11:36 AM
K 2440 Orthaclase 2-Dec-2010 04:33 PM
Ti 2440 Ti 2-Dec-2010 03:56 PM
Fe 3587 AISI 316 14-Dec-2010 02:09 PM

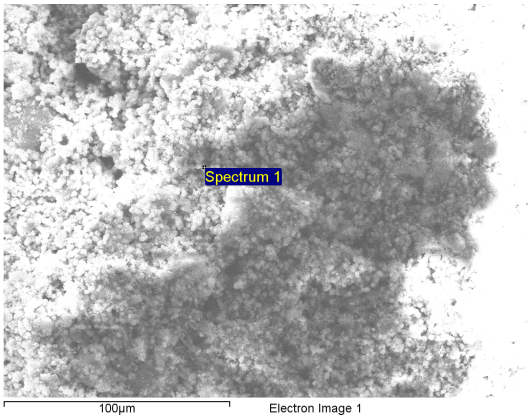

Element	Weight%	Atomic%
O K	44.95	60.08
Na K	2.82	2.62
Mg K	0.32	0.28
Al K	8.56	6.79
Si K	33.71	25.67
S K	1.62	1.08
K K	2.30	1.26
Ti K	0.59	0.26
Fe K	5.14	1.97
Totals	100.00	

Figure B9: Askja 1875 94-day experiment, wall scales.

Na-rich Si-Al phase with Ca and K.
Probably Na-montomorillonite.
Processing option All elements analyzed (Normalised)
Number of iterations = 3
Standard:
O 2440 CaCO3 3-Nov-2010 02:54 PM
Na 2440 Altite 2-Dec-2010 04:15 PM
Al 2440 Altite 2-Dec-2010 04:14 PM
Si 3587 AISI 316 14-Dec-2010 02:09 PM
K 2440 Orthaclase 2-Dec-2010 04:33 PM
Ca 2440 Diopside 2-Dec-2010 05:18 PM

Element	Weight%	Atomic%
O K	50.84	64.57
Na K	0.93	0.82
Al K	1.24	0.93
Si K	45.42	32.86
K K	0.67	0.35
Ca K	0.90	0.46
Totals	100.00	

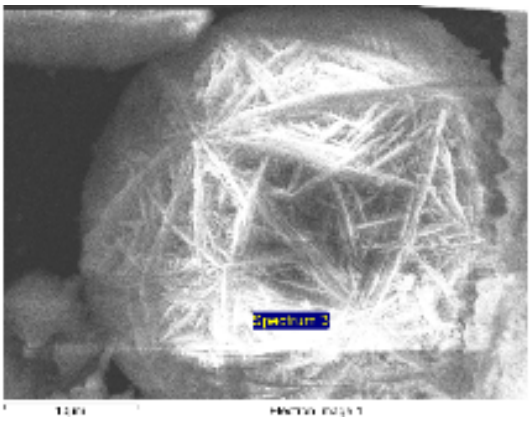

Figure B10: Hekla H3W 42-day experiment, wall scales.

Na-rich zeolite, with some K as well.
Probably analcime
Processing option: All elements analyzed (Normalised)
Number of iterations = 4
Standard:
C 2440 CaCO3 3-Nov-2010 02:54 PM
O 2440 CaCO3 3-Nov-2010 02:54 PM
Na 2440 Altite 2-Dec-2010 04:15 PM
Al 2440 Altite 2-Dec-2010 04:14 PM
Si 3587 AISI 316 14-Dec-2010 02:09 PM
K 2440 Orthaclase 2-Dec-2010 04:33 PM

Element	Weight%	Atomic%
C K	2.86	4.82
O K	46.56	58.76
Na K	0.72	0.63
Al K	0.76	0.57
Si K	48.75	35.04
K K	0.35	0.18
Totals	100.00	

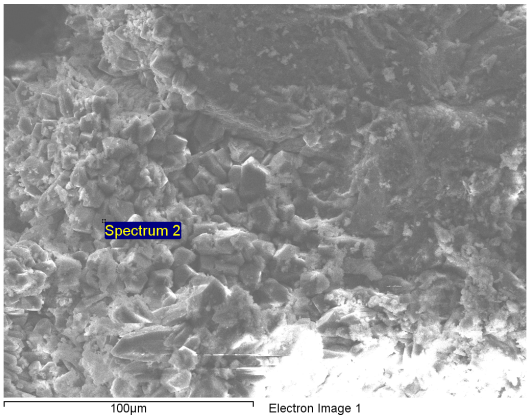

Figure B11: Askja 1875 94-day experiment, wall scales.

Amorphous silica
Processing option: All elements analyzed (Normalised)
Number of iterations = 3
Standard:
O 2440 CaCO3 3-Nov-2010 02:54 PM
Si 3587 AISI 316 14-Dec-2010 02:09 PM

Element	Weight%	Atomic%
O K	55.93	69.02
Si K	44.07	30.98
Totals	100.00	

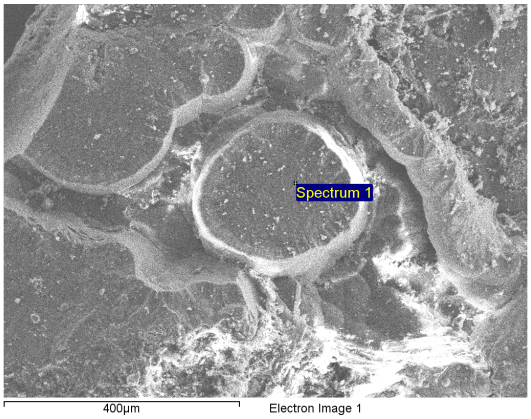

Figure B12: Askja 1875 94-day experiment, bulk material.

Fe-rich Si-Al phase with K and Mg. Smectite/chlorite.
Processing option: All elements analyzed (Normalised)
Number of iterations = 4
Standard:
C 2440 CaCO3 3-Nov-2010 02:54 PM
O 2440 CaCO3 3-Nov-2010 02:54 PM
Na 2440 Altite 2-Dec-2010 04:15 PM
Mg 2440 Diopside 2-Dec-2010 04:29 PM
Al 2440 Altite 2-Dec-2010 04:14 PM
Si 3587 AISI 316 14-Dec-2010 02:09 PM
K 2440 Orthaclase 2-Dec-2010 04:33 PM
Ca 2440 Diopside 2-Dec-2010 05:18 PM
Ti 2440 Ti 2-Dec-2010 03:56 PM
Fe 3587 AISI 316 14-Dec-2010 02:09 PM

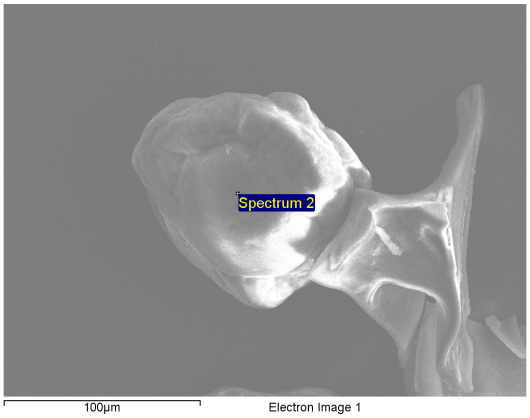

Element	Weight%	Atomic%
C K	0.98	1.80
O K	42.33	58.06
Na K	0.91	0.87
Mg K	2.16	1.95
Al K	7.57	6.16
Si K	31.66	24.74
K K	3.37	1.89
Ca K	0.89	0.49
Ti K	1.14	0.52
Fe K	8.98	3.53
Totals	100.00	

Figure B13: Askja 1875 94-day experiment, bulk material.

This Fe-rich Si-Al phase contains appreciable amounts of Ti, probably in the form of anatase (TiO_2).
Processing option: All elements analyzed (Normalised)
Number of iterations = 2
Standard:
O 2440 CaCO3 3-Nov-2010 02:54 PM
Na 2440 Altite 2-Dec-2010 04:15 PM
Al 2440 Altite 2-Dec-2010 04:14 PM
Si 3587 AISI 316 14-Dec-2010 02:09 PM
Ca 2440 Diopside 2-Dec-2010 05:18 PM
Ti 2440 Ti 2-Dec-2010 03:56 PM
Fe 3587 AISI 316 14-Dec-2010 02:09 PM

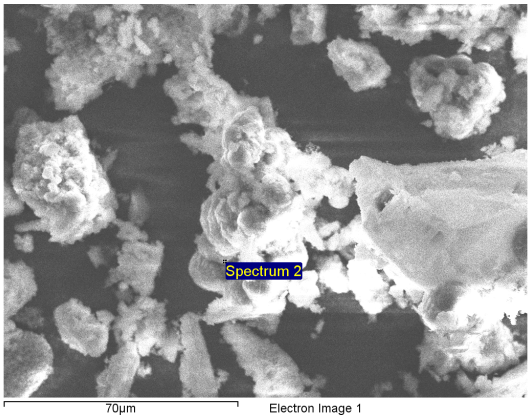

Element	Weight%	Atomic%
O K	10.58	24.54
Na K	1.24	2.01
Al K	3.10	4.27
Si K	16.32	21.56
Ca K	5.21	4.82
Ti K	5.26	4.08
Fe K	58.29	38.73
Totals	100.00	

Figure B14: Hekla H3W 42-day experiment, bulk material.

Fe-rich Si-Al phase with considerable amounts of K. Probably mixed illite-smectite.
Processing option: All elements analyzed (Normalised)
Number of iterations = 3
Standard:
O 2440 CaCO3 3-Nov-2010 02:54 PM
Na 2440 Altite 2-Dec-2010 04:15 PM
Al 2440 Altite 2-Dec-2010 04:14 PM
Si 3587 AISI 316 14-Dec-2010 02:09 PM
K 2440 Orthaclase 2-Dec-2010 04:33 PM
Ca 2440 Diopside 2-Dec-2010 05:18 PM
Ti 2440 Ti 2-Dec-2010 03:56 PM
Fe 3587 AISI 316 14-Dec-2010 02:09 PM
Au Au 1-Jun-1999 12:00 AM

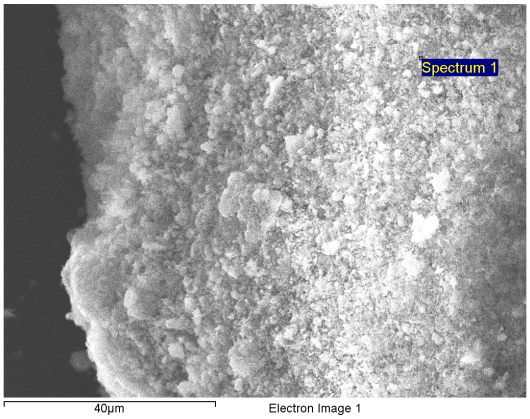

Element	Weight%	Atomic%
O K	32.38	50.32
Na K	2.07	2.24
Al K	8.43	7.77
Si K	31.03	27.47
K K	3.51	2.23
Ca K	1.88	1.17
Ti K	3.09	1.60
Fe K	15.59	6.94
Au M	2.01	0.25
Totals	100.00	

Figure B15: Hekla H3W 42-day experiment, bulk material.

Ca-Si phase with a small amount of fluorite.
Processing option: All elements analyzed (Normalised)
Number of iterations = 4
Standard:
C 2440 CaCO3 3-Nov-2010 02:54 PM
O 2440 CaCO3 3-Nov-2010 02:54 PM
F 3587 ALF3 10-Dec-2009 11:40 AM
Na 2440 Altite 2-Dec-2010 04:15 PM
Si 3587 AISI 316 14-Dec-2010 02:09 PM
K 2440 Orthaclase 2-Dec-2010 04:33 PM
Ca 2440 Diopside 2-Dec-2010 05:18 PM

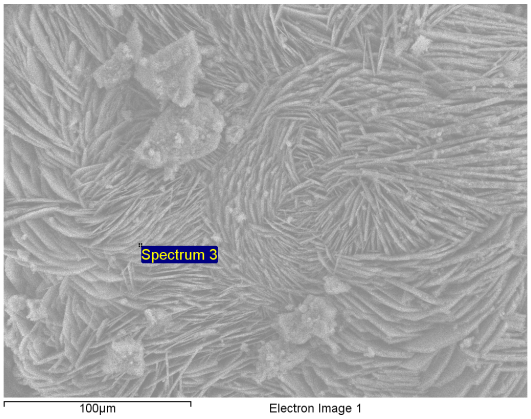

Element	Weight%	Atomic%
C K	0.62	1.14
O K	38.49	53.48
F K	1.25	1.47
Na K	2.25	2.18
Si K	41.78	33.07
K K	0.83	0.47
Ca K	14.77	8.19
Totals	100.00	

Appendix C. The logarithms of the activities of various species, calculated with PHREEQC program and llnl.dat database

Sample	days	pH	E_h	Alk	H^+	H_4SiO_4	Na^+	K^+	Ca^{2+}	Mg^{2+}	Al^{+3}	AlO_2^-	Fe^{2+}	Fe^{3+}	$Fe(OH)_4^-$	HCO_3^-	H_2S	SO_4^{2-}	F^-	$H_2(aq)$
			Volt	meq/kg																
Askja 1875 (A75) material - 94 day experiment																				
1	1	6.45	-0.34	5.42	-6.45	-1.96	-1.22	-2.82	-4.90	-7.40	-20.58	-4.70	-4.83	-20.21	-16.00	-2.49	-4.18	-3.36	-3.99	-5.76
2	10	6.40	-0.34	4.62	-6.40	-1.87	-1.23	-2.48	-4.72	-7.50	-20.73	-5.09	-5.55	-20.86	-16.89	-2.56	-4.17	-3.45	-3.64	-5.76
3	20	6.62	-0.37	4.86	-6.62	-1.86	-1.23	-2.37	-4.62	-7.88	-21.84	-5.31	-5.73	-21.34	-16.47	-2.55	-4.26	-3.63	-3.53	-5.63
4	31	6.89	-0.40	3.08	-6.89	-1.86	-1.26	-2.29	-4.44	-7.68	-22.98	-5.38	-6.03	-21.99	-16.05	-2.80	-4.36	-3.85	-3.50	-5.47
5	41	6.93	-0.41	3.38	-6.93	-1.93	-1.26	-2.26	-4.45	-7.76	-23.23	-5.44	-6.23	-22.25	-16.12	-2.75	-4.38	-3.85	-3.58	-5.45
6	52	6.40	-0.34	2.58	-6.40	-2.06	-1.26	-2.21	-4.40	-8.33	-20.96	-5.32	-6.31	-21.69	-17.72	-2.82	-4.06	-3.86	-3.70	-5.63
7	62	6.83	-0.40	3.40	-6.83	-2.09	-1.27	-2.19	-4.43	-7.78	-22.62	-5.25	-6.32	-22.21	-16.50	-2.72	-4.32	-3.85	-3.80	-5.48
8	73	6.72	-0.38	3.01	-6.72	-2.21	-1.26	-2.11	-4.34	-7.18	-21.90	-4.95	-6.12	-21.89	-16.61	-2.78	-4.22	-3.86	-3.88	-5.51
10	94	6.63	-0.37	2.12	-6.63	-2.28	-1.33	-2.12	-4.37	-7.53	-21.31	-4.73	-6.15	-21.82	-16.90	-2.94	-4.22	-3.96	-4.10	-5.53
Askja 1875 (A75) material - 30 day experiment																				
1	0	7.08	-0.43	8.90	-7.08	-2.22	-1.21	-3.02	-5.43	-7.87	-22.49	-4.13	-6.16	-22.41	-15.72	-2.32	-3.91	-3.83	-4.40	-5.26
2	5	7.00	-0.42	6.76	-7.00	-1.95	-1.22	-2.61	-5.27	-7.73	-22.62	-4.55	-6.54	-22.62	-16.22	-2.42	-4.44	-3.82		-5.43
3	10	6.86	-0.39	5.89	-6.86	-1.94	-1.23	-2.52	-5.03	-7.33	-22.11	-4.61	-6.08	-21.95	-16.12	-2.47	-4.72	-3.79	-3.82	-5.58
4	15	6.92	-0.40	5.98	-6.92	-1.91	-1.23	-2.47	-5.04	-7.63	-22.48	-4.74	-6.61	-22.56	-16.48	-2.47	-4.70	-3.77	-3.84	-5.55
5	20	6.86	-0.39	5.11	-6.86	-1.90	-1.22	-2.44	-4.95	-7.25	-22.34	-4.86	-6.58	-22.44	-16.61	-2.54	-4.74	-3.75	-3.80	-5.60
6	25	7.02	-0.41	6.81	-7.02	-1.86	-1.20	-2.40	-4.93	-7.75	-22.80	-4.65	-6.53	-22.59	-16.10	-2.43	-4.77	-3.73	-3.77	-5.53
7	30	7.09	-0.42	6.94	-7.09	-1.90	-1.22	-2.40	-4.96	-7.63	-23.26	-4.85	-6.47	-22.61	-15.86	-2.41	-4.80	-3.75	-3.75	-5.50
Hekla (H3W) material - 42-day experiment of																				
1	0	6.99	-0.41	11.21	-6.99	-2.13	-1.23	-2.64	-5.02	-7.05	-22.08	-4.08	-6.29	-22.33	-15.99	-2.19	-4.56	-3.70	-3.51	-5.50
2	5	7.01	-0.42	11.61	-7.01	-1.92	-1.23	-2.46	-5.29	-7.80	-22.49	-4.38	-6.47	-22.64	-16.19	-2.18	-3.86	-3.77		-5.30
3	10	6.91	-0.41	9.28	-6.91	-1.99	-1.24	-2.46	-5.03	-7.55	-21.73	-4.02	-6.43	-22.51	-16.46	-2.31	-3.62	-3.78	-3.04	-5.29
4	15	6.97	-0.42	8.62	-6.97	-1.98	-1.22	-2.44	-5.12	-7.45	-22.07	-4.13	-6.46	-22.61	-16.34	-2.35	-3.57	-3.77	-3.03	-5.25
5	20	7.21	-0.45	9.14	-7.21	-2.02	-1.23	-2.45	-5.20	-7.73	-23.16	-4.26	-6.80	-23.23	-15.99	-2.33	-3.79	-3.78	-3.05	-5.18
6	25	7.29	-0.46	9.16	-7.29	-2.02	-1.24	-2.47	-5.32	-8.01	-23.60	-4.37	-7.03	-23.55	-15.97	-2.32	-3.91	-3.78	-3.06	-5.16
7	31	7.39	-0.47	9.59	-7.39	-1.96	-1.22	-2.44	-5.34	-8.10	-24.07	-4.43	-7.10	-23.73	-15.76	-2.32	-3.99	-3.78	-3.04	-5.14
8	42	7.27	-0.46	6.67	-7.27	-1.90	-1.20	-2.31	-4.92	-8.46	-24.17	-5.02	-6.87	-23.34	-15.86	-2.49	-4.01	-3.78	-3.19	-5.20

Appendix D. Mineral saturation indices (SI)

Sample	qtz	am-Si	boh	cc	flu	anh	anl	wai	mont	ill	alb	mic	pyr	mt	hem	chl	epi	czo	pre
Askja 1875 (A75) material - 94 day experiment																			
1	0.20	-0.27	0.00	0.19	-1.46	-0.04	0.12	0.23	1.38	0.91	1.60	0.99	3.81	-9.80	-13.81	-2.29	-4.80	2.24	1.70
2	0.29	-0.18	-0.33	0.25	-0.58	0.05	-0.08	0.00	1.10	0.59	1.48	1.21	2.99	-12.30	-15.48	-3.22	-5.88	1.67	1.45
3	0.30	-0.17	-0.78	0.58	-0.25	-0.03	-0.26	-0.29	0.51	-0.17	1.30	1.14	2.94	-11.66	-15.09	-2.78	-5.46	1.45	1.68
4	0.30	-0.17	-1.11	0.78	-0.03	-0.06	-0.35	-0.23	0.29	-0.54	1.21	1.16	2.81	-11.12	-14.79	1.64	-4.53	1.89	2.46
5	0.23	-0.24	-1.22	0.87	-0.19	-0.07	-0.57	-0.67	-0.19	-1.00	0.92	0.90	2.65	-11.45	-15.01	1.42	-4.92	1.51	2.19
6	0.10	-0.37	-0.56	0.30	-0.39	-0.05	-0.72	-0.91	-0.33	-0.65	0.65	0.68	2.32	-14.72	-17.13	-8.95	-7.12	1.03	1.04
7	0.07	-0.40	-0.92	0.80	-0.61	-0.06	-0.72	-0.90	-0.44	-0.95	0.62	0.69	2.51	-12.29	-15.56	-0.59	-5.46	1.54	1.91
8	-0.05	-0.52	-0.52	0.72	-0.68	0.02	-0.65	-0.69	-0.13	-0.35	0.59	0.72	2.72	-12.32	-15.57	1.28	-5.26	2.14	2.12
10	-0.12	-0.59	-0.21	0.45	-1.14	-0.10	-0.67	-0.58	-0.15	-0.10	0.50	0.69	2.53	-12.94	-15.98	-2.23	-5.49	2.43	2.10
Askja 1875 (A75) material - 30 day experiment																			
1	-0.06	-0.53	-0.05	0.46	-2.81	-1.03	0.16	-0.16	0.76	0.36	1.43	0.60	3.77	-10.57	-14.49	1.33	-4.56	2.77	2.28
2	0.21	-0.26	-0.40	0.44	6.15	-0.88	0.29	0.21	1.20	0.69	1.79	1.39	2.35	-11.96	-15.36	2.37	-4.88	2.54	2.39
3	0.22	-0.25	-0.31	0.49	-1.24	-0.60	0.25	0.38	1.37	0.92	1.76	1.45	2.11	-11.30	-14.87	3.08	-4.52	2.74	2.51
4	0.25	-0.22	-0.51	0.54	-1.30	-0.59	0.18	0.21	1.13	0.60	1.71	1.45	1.72	-12.55	-15.71	2.15	-5.02	2.47	2.43
5	0.26	-0.21	-0.56	0.50	-1.13	-0.49	0.10	0.12	1.16	0.57	1.64	1.40	1.59	-12.78	-15.85	3.72	-5.24	2.27	2.28
6	0.30	-0.17	-0.52	0.80	-1.04	-0.44	0.41	0.74	1.41	0.90	2.00	1.79	1.84	-11.71	-15.16	2.90	-3.96	3.24	3.21
7	0.26	-0.21	-0.79	0.84	-1.04	-0.48	0.12	0.15	0.90	0.25	1.67	1.46	1.94	-11.17	-14.81	4.21	-4.24	2.52	2.76
Hekla (H3W) material - 42-day experiment of																			
1	0.03	-0.44	0.09	0.91	-0.61	-0.50	0.36	0.69	1.50	1.32	1.71	1.29	2.39	-11.25	-14.86	5.55	-3.75	3.91	3.28
2	0.24	-0.23	-0.24	0.67	6.13	-0.85	0.51	0.66	1.59	1.26	2.06	1.81	3.46	-11.83	-15.32	2.20	-4.44	3.12	2.81
3	0.17	-0.30	0.22	0.71	0.31	-0.58	0.71	1.38	2.07	2.04	2.20	1.96	3.76	-12.33	-15.66	2.22	-3.76	4.44	3.67
4	0.18	-0.29	0.05	0.63	0.24	-0.67	0.63	1.09	1.90	1.77	2.13	1.89	3.91	-12.13	-15.53	3.55	-3.97	3.99	3.39
5	0.14	-0.33	-0.32	0.82	0.11	-0.76	0.41	0.57	1.25	0.95	1.86	1.62	3.54	-11.76	-15.31	4.56	-3.93	3.55	3.32
6	0.14	-0.33	-0.51	0.78	-0.02	-0.88	0.31	0.25	0.93	0.53	1.75	1.50	3.24	-11.96	-15.45	3.93	-4.28	3.08	3.04
7	0.20	-0.27	-0.67	0.86	0.00	-0.90	0.38	0.35	0.98	0.47	1.88	1.65	3.17	-11.59	-15.21	4.80	-3.94	3.13	3.26
8	0.26	-0.21	-1.14	0.99	0.11	-0.48	-0.05	-0.19	0.19	-0.55	1.49	1.36	3.19	-11.56	-15.17	1.41	-4.34	2.24	2.84